

Causal Bayesian Optimization via Exogenous Distribution Learning

Shaogang Ren Xiaoning Qian

Department of Electrical and Computer Engineering
Texas A&M University

Abstract

Maximizing a target variable as an operational objective in a structural causal model is an important problem. Existing Causal Bayesian Optimization (CBO) methods either rely on hard interventions that alter the causal structure to maximize the reward; or introduce action nodes to endogenous variables so that the data generation mechanisms are adjusted to achieve the objective. In this paper, a novel method is introduced to learn the distribution of exogenous variables, which is typically ignored or marginalized through expectation by existing methods. Exogenous distribution learning improves the approximation accuracy of structural causal models in a surrogate model that is usually trained with limited observational data. Moreover, the learned exogenous distribution extends existing CBO to general causal schemes beyond Additive Noise Models (ANM). The recovery of exogenous variables allows us to use a more flexible prior for noise or unobserved hidden variables. We develop a new CBO method by leveraging the learned exogenous distribution. Experiments on different datasets and applications show the benefits of our proposed method.

1 Introduction

Bayesian Optimization (BO) has broad applications, such as automating modern industrial processes, drug discovery, and more general synthetic biology, that require optimizing black-box objective functions [16; 3]. In many real-world problems, we have some structural knowledge of the unknown functions that can be leveraged to improve BO efficiency. Causal Bayesian Optimization (CBO) has been developed to utilize the structural information of the objective [2; 1; 23]. CBO combines ideas from causal inference, uncertainty quantification, and sequential decision-making. It generalizes Bayesian Optimization, which treats the input variables of the objective function as independent, to

scenarios where causal information between input variables is available [2]. CBO has been developed for optimizing medical and ecological interventions as illustrative examples [2; 1].

1.1 Approach and Contributions

In this paper, we develop a Causal Bayesian Optimization method, EXCBO. Given observation data points of a structural causal model (SCM), the exogenous variable associated with each endogenous node is recovered with an encoder-decoder framework. The learned distribution of the exogenous variable is then approximated with the density of the recovered exogenous variable that is parameterized with a flexible model, e.g. Gaussian Mixture. The recovered exogenous distribution improves the surrogate model’s accuracy in the SCM approximation. Different from existing CBO methods [2; 1; 23] that typically focus on Additive Noise Models (ANMs, [12]), our method enables us to extend CBO to general causal models beyond ANMs. Our flexible surrogate model has the benefit of better causal inference regarding CBO updating.

The contributions in this paper include

- We propose a method to recover the exogenous noise variable of each endogenous node in an SCM using observational data; the exogenous distribution in each node is then learned using a flexible model that is capable of modeling multi-mode density functions;
- We develop a Causal Bayesian Optimization algorithm leveraging the learned exogenous distribution (EXCBO), where the flexibility of learning exogenous distributions naturally extends the proposed CBO framework to general causal models beyond ANMs.
- We provide a theoretical study on the recovery of exogenous variables. Moreover, we give a theoretical analysis of the algorithm regret bound. Our analysis shows that the proposed EXCBO algorithm achieves sublinear cumulative regret bounds.
- Experiments have been performed to validate the benefits of exogenous distribution learning and the proposed EXCBO algorithm. Applications on epidemic dynamic model calibration are discussed to support the proposed CBO framework.

In the following parts of this paper, Section 2 presents the background and related work; Section 3 sets up the problem studied in this paper with the introduction of the proposed CBO framework; Section 4 presents the exogenous recovery method; The proposed SCM algorithm, EXCBO, is detailed in Section 5 with theoretical analysis of EXCBO given in Section 6; Section 7 presents experimental results; Section 8 concludes the paper.

2 Background and Related Work

We first review causal inference and Causal Bayesian Optimization (CBO).

2.1 Structural Causal Model

A structural causal model (SCM, [19; 20]) is denoted by $\mathcal{M} = (\mathcal{G}, \mathbf{F}, \mathbf{X}, \mathbf{U})$. Here \mathcal{G} is a directed acyclic graph (DAG), and $\mathbf{F} = \{\mathbf{f}_i\}_{i=0}^d$ stands for d mechanisms of all variables. \mathbf{X} is the endogenous variable set, and \mathbf{U} is the exogenous (background) variable set. Samples of the i th endogenous

variable are generated with

$$\begin{aligned} X_i &= \mathbf{f}_i(Z_i, U_i), \text{ with } U_i \sim p(U_i), \\ Z_i &= \mathbf{pa}(i) \text{ for } i = 1, \dots, d. \end{aligned} \quad (1)$$

We use X_i to represent the i th variable as well as the i th node in \mathcal{G} . $\mathbf{pa}(i)$ and $\mathbf{ch}(i)$ are the parent and child set of node X_i , respectively; \mathbf{f}_i is a mapping from $\mathbb{R}^{|\mathbf{pa}(i)|+1} \rightarrow \mathbb{R}$; Moreover, \mathcal{X}_i and \mathcal{Z}_i stand for the value range of X_i and Z_i , respectively.

In our proposed CBO algorithm, we assume that the data generation mechanism in one node is given by (1). Different from (1), existing CBO methods [2; 23] usually assume that the exogenous variable is an additive noise (ANM, [12]) to the data generation mechanism, i.e.,

$$X_i = \mathbf{f}_i(Z_i) + U_i, \text{ with } U_i \sim \mathcal{N}(0, 1).$$

Furthermore, existing methods also assume that the exogenous variables follow Gaussian distributions. In contrast, the SCMs in this work are not limited by these restricted assumptions. Each U_i can be non-Gaussian and has multiple modes. Hence the SCMs in our work are more general and may have broader real-world applications.

Following existing CBO algorithms [2; 1; 23], the DAG \mathcal{G} is assumed to be known, and learning of its structure is left for future work in integration with causal discovery [11] methods.

2.2 Intervention

In SCM \mathcal{M} , let \mathbf{I} be a subset of endogenous variables, i.e. $\mathbf{I} \subset \mathbf{X}$. The intervention on target \mathbf{I} is given by

$$\mathbf{F}_{\mathbf{x}} = \{\mathbf{f}_i | X_i \notin \mathbf{I}\} \cup \{\mathbf{f}'_j | X_j \in \mathbf{I}\}.$$

The intervention on variable X_j is implemented with the change of the data generation mechanism from \mathbf{f}_i to \mathbf{f}'_i . There are generally two types of interventions: hard and soft intervention.

The hard intervention on target \mathbf{I} is given by

$$\mathbf{F}_{\mathbf{x}} = \{\mathbf{f}_i | X_i \notin \mathbf{I}\} \cup \{\mathbf{f}'_j := \boldsymbol{\alpha}_j | X_j \in \mathbf{I}\}.$$

Here $\boldsymbol{\alpha}$ is the realization of variables in \mathbf{I} . The do-operation [19] $do(\mathbf{X} := \boldsymbol{\alpha})$ represents the hard intervention that changes the SCM from \mathcal{M} to $\mathcal{M}_{\boldsymbol{\alpha}}$. A hard intervention on a node breaks its causal connection with its parents. The submodel $\mathcal{M}_{\boldsymbol{\alpha}}$ is the SCM with the same exogenous and endogenous variables and prior distributions over \mathbf{U} as \mathcal{M} .

This paper focuses on the soft intervention (or, imperfect intervention) [21]. Following MCBO [23], we introduce an action variable to each endogenous variable, i.e.,

$$\mathbf{F}_{\mathbf{x}} = \{\mathbf{f}_i | X_i \notin \mathbf{I}\} \cup \{\mathbf{f}'_j := \mathbf{f}'_j(Z_j, A_j, U_j) | X_j \in \mathbf{I}\}. \quad (2)$$

Here $Z_j = \mathbf{pa}(j)$. With the soft intervention on target \mathbf{I} , the data generation mechanism becomes

$$X_i = \begin{cases} \mathbf{f}_i(Z_i, U_i), & \text{if } X_i \notin \mathbf{I} \\ \mathbf{f}'_i(Z_i, A_i, U_i), & \text{if } X_i \in \mathbf{I} \end{cases}, \quad (3)$$

where A_i is the continuous action variable for X_i if $X_i \in \mathbf{I}$. Action A_i controls the change of the data generation mechanism of node X_i .

Existing CBO methods often use Gaussian Processes (GPs) as probabilistic surrogate models to search for the intervention target set and the corresponding realization or action values. CBO methods [2; 1] search for hard interventions in pursuit of the optimal objective; however, MCBO [23] optimizes the soft interventions on an SCM to achieve the maximum of the target variable. In the initial steps of MCBO, the intervention target \mathbf{I} includes almost all the nodes except the target node.

2.3 Function Network Bayesian Optimization

Similar to CBO, the structure of the functions in Function Network BO (FNBO, [4; 3]) is assumed to be given, and the parameters and specific form of each function are unknown. FNBO operates soft interventions and uses an expected improvement (EI) acquisition function to select actions. FNBO assumes that the system is noiseless, which could be a restrictive assumption in practice. In this paper, we take a function network with noise observations as an SCM, and the independent noises are exogenous variables. Both FNBO and CBO belong to a broad research direction using intermediate observations from the computation of the unknown functions to improve the sample efficiency of vanilla BO algorithms [5].

2.4 Causal Bayesian Optimization

In this subsection, we give a brief review of Causal Bayesian Optimization (CBO) [2; 1; 23]. In CBO, a sequence of actions is performed to interact with a structural causal model (SCM) \mathcal{M} . The DAG \mathcal{G} in \mathcal{M} is given, with the edge functions $\mathbf{F} = \{\mathbf{f}_i\}_{i=0}^d$ being fixed but unknown. Probabilistic surrogate models are implemented to search for the intervention actions in attaining the optimal objective/reward value.

In [2], the authors proposed a CBO algorithm that obtains both the optimal intervention target set and the corresponding input values to reach the optimal objective value in an SCM. The algorithm in [2] utilizes the expected improvement (EI) algorithm and GP surrogate model to get the hard intervention set that maximizes the objective or reward variable.

A dynamic CBO (DCBO) algorithm is proposed in [1], where all causal effects in the SCM \mathcal{M} are changing over time. At every time step DCBO identifies a local optimal intervention by integrating both observational and past interventional data collected from the system.

In MCBO [23], soft interventions are optimized to achieve the maximum target variable in an SCM. The edge function set is $\mathbf{F} = \{\mathbf{f}_i\}_{i=1}^d$ with $\mathbf{f}_i : \mathcal{Z}_i \times \mathcal{A}_i \rightarrow \mathcal{X}_i$. Let $\mathbf{x}_{i,t}$ denotes the observation of node X_i at time step t , and $i \in [d]$, $t \in [T]$. T is the total number of time steps. At step t MCBO selects actions $\mathbf{a}_{:t} = \{\mathbf{a}_{i,t}\}_0^d$ and obtains observations $\mathbf{x}_{:,t} = \{\mathbf{x}_{i,t}\}_0^d$. The relation between the action $\mathbf{a}_{i,t}$ and the observation is given by an additive noise model, i.e.,

$$\mathbf{x}_{i,t} = \mathbf{f}_i(\mathbf{z}_{i,t}, \mathbf{a}_{i,t}) + \mathbf{u}_{i,t}, \quad \forall i \in [d].$$

At the target node d , $\mathbf{a}_{d,t} = 0$, and

$$y_t = \mathbf{f}_d(\mathbf{z}_{d,t}, \mathbf{a}_{d,t}) + \mathbf{u}_{d,t},$$

and here y_t depends on the whole intervention vector. The action vector that maximizes the expected reward regarding the exogenous variable, i.e.,

$$\mathbf{a}^* = \arg \max_{\mathbf{a} \in \mathcal{A}} \mathbb{E}[y|\mathbf{a}]. \quad (4)$$

GP surrogate model is implemented to learn the reward function to guide BO to optimize y .

3 Problem Statement

Compared to existing methods, our proposed CBO framework studies more general causal models as given in (1). Similar to MCBO [23], our framework adopts GP surrogate models to guide the optimization of soft interventions controlled by an action vector $\mathbf{a} = \{\mathbf{a}_i\}_{i=0}^d$ in reaching the optimal reward value. This section gives additional details about the problem settings studied in this paper.

3.1 Regularity Assumption

In our problem, the edges in SCM \mathcal{M} is a fixed but unknown set of functions $\mathbf{F} = \{\mathbf{f}_i\}_{i=1}^d$ with $\mathbf{f}_i : \mathcal{Q} \rightarrow \mathcal{X}_i$. We consider standard smoothness assumptions for the unknown functions \mathbf{f}_i defining over a compact domain \mathcal{Q} [22]. For each node $i \in [d]$, we assume that $\mathbf{f}_i(\cdot)$ belongs to a reproducing kernel Hilbert space (RKHS) \mathcal{H}_k , a space of smooth functions defined on $\mathcal{Q} = \mathcal{Z}_i \times \mathcal{A}_i \times \mathcal{U}_i$. This means that $\mathbf{f}_i \in \mathcal{H}_k$ is induced by a kernel function $k_i : \mathcal{Q} \times \mathcal{Q} \rightarrow \mathbb{R}$. We also assume that $k_i(s, s') \leq 1$ for every $s, s' \in \mathcal{Q}$. The RKHS norm of $\mathbf{f}_i(\cdot)$ is assumed to be bounded $\|\mathbf{f}_i\|_{k_i} \leq \mathcal{B}_i$ for some fixed constant $\mathcal{B}_i > 0$ [23].

We further assume that \mathcal{A}_i and $\mathcal{U}_i, i \in [d]$ are compact and bounded. The intervention target set \mathbf{I} is assumed to a subset of \mathbf{X} , i.e., $|\mathbf{I}| < d - 1$.

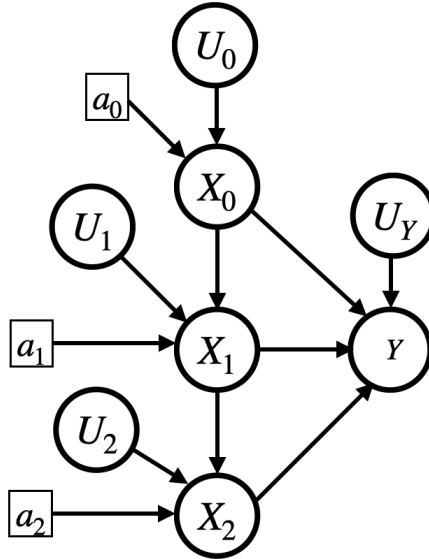


Figure 1: **EXCBO**: Causal Bayesian Optimization through exogenous distribution learning. The distribution of U_i is approximated with the density of recovered values of U_i . The CBO algorithm searches for the action vector \mathbf{a} that maximizes the reward Y .

3.2 CBO via Exogenous Distribution Learning

Different from the Additive Noise Models (ANMs) in existing CBO algorithms, such as MCBO [23], we here propose to flexibly model the mapping $\mathbf{f}_i(\cdot)$ with introduced exogenous variables, for which we propose a new EXCBO framework for CBO through exogenous distribution learning. At step t

of CBO, the relation between actions $\mathbf{a}_{i,t}$, $\mathbf{u}_{i,t}$ and the observation $\mathbf{x}_{i,t}$ is given by

$$\mathbf{x}_{i,t} = \mathbf{f}_i(\mathbf{z}_{i,t}, \mathbf{a}_{i,t}, \mathbf{u}_{i,t}) \quad \forall i \in [d]. \quad (5)$$

Our surrogate model in EXCBO takes the exogenous variable U_i as the input as shown in (5). In our SCMs, the exogenous variables are not simply noise in the system. We assume they are important background or environmental factors that affect the output of the SCM. Using an example in biology, $\mathbf{x}_{i,t}$ is the community size of a species of bacteria at time t , and $\mathbf{u}_{i,t}$ can be the amount of a chemical compound in the environment that affects the growth of the bacteria but independent with other factors and also unknown to us.

Let \mathcal{R} represent the root node set. As the parent of root nodes is null, we set $\mathbf{z}_{i,t} = \mathbf{0}$, if $i \in \mathcal{R}$. Similarly, we have $\mathbf{a}_{d,t} = 0$ at the target node d ,

$$y_t = \mathbf{f}_d(\mathbf{z}_{d,t}, \mathbf{a}_{d,t}, \mathbf{u}_{d,t}).$$

Given an action vector $\mathbf{a} = \{\mathbf{a}_i\}_{i=0}^d$ and $\mathbf{u} = \{\mathbf{u}_i\}_{i=0}^d$, the reward or target value is simply denoted with $y = \mathbf{F}(\mathbf{a}, \mathbf{u})$. The problem becomes searching for an action vector maximizing the objective, i.e.,

$$\mathbf{a}^* = \arg \max_{\mathbf{a} \in \mathcal{A}} \mathbb{E}[y|\mathbf{a}], \quad (6)$$

where the expectation is to take over \mathbf{u} . The goal of our method is to design a sequence of interventions $\{\mathbf{a}_{t=0}^T\}$ that achieves a high average expected reward. Following [23]. The learning of exogenous variable distribution provides a more accurate surrogate model given an SCM and observational data.

To analyze the convergence of our method, we study the cumulative regret over a time horizon T :

$$R_T = \sum_{t=1}^T \left[\mathbb{E}[y|\mathbf{a}^*] - \mathbb{E}[y|\mathbf{a}_{:,t}] \right].$$

Cumulative regret bound helps us to analyze the convergence of the algorithm. In the experiments, we use the attained objective value or reward value y as the metric to compare our method and existing algorithms. A better metric depends on the real-world application and the effectiveness of the optimized action sequence.

3.3 Motivations for Exogenous Distribution Learning

In existing CBO models, exogenous distributions are ignored or marginalized to achieve the simplicity of interventions [2; 1; 23]. As mentioned in previous sections, we propose an encoder-decoder scheme to recover the exogenous variable of each endogenous node in an SCM. The distribution of the exogenous variable (U), is approximated with the density of the recovered exogenous variable (\hat{U}) which is modeled with a flexible model, e.g. Gaussian Mixture. The recovered exogenous distribution improves the surrogate model in the approximation of the SCM. Different from existing methods [2; 1; 23] that typically rely on the ANM assumption, our EXCBO allows us to extend CBO to a broader range of causal models beyond ANMs. With a more accurate surrogate model, our method could achieve improved reward and objective values.

4 Exogenous Distribution Learning

Given the observations of an endogenous node and its parents in an SCM, our method is to recover the distribution of the node’s endogenous variable. The learning of the exogenous distribution is implemented with the Gaussian Process. We first focus on the exogenous distribution learning regarding one node.

4.1 Exogenous Variable Recovery in One Node

According to (3), an endogenous variable X_i either has an action variable A_i or not. To better illustrate the idea with compact notations, we use Z_i to represent variable X_i ’s parents and its action variable in this section (Section 4), i.e., $Z_i = (Z_i, A_i)$ if $X_i \in \mathbf{I}$. Hence the learning of node X ’s exogenous distortion becomes a problem of recovering U ’s distribution given the observations of X and Z regarding equation $X = \mathbf{f}(Z, U)$. To make our presentation concise, we have the following definition for the causal mechanism of the triplets (Z, U, X) that appear as a node in an SCM.

Definition 4.1. (τ -SCM) *Let X and U be one-dimensional variables, and $\mathbf{f}()$ is the causal mechanism generating X from variables Z and U , i.e. $X = \mathbf{f}(Z, U)$. We assume $Z \perp\!\!\!\perp U$, and (Z, U, X, \mathbf{f}) is defined as a τ -SCM.*

In a τ -SCM, Z is the parent of X , and it may be multi-dimensional; U is the exogenous variable of X . Different from the bijective generation mechanisms (BGM) [17], $\mathbf{f}()$ is not confined to be monotonic and invertible regarding X and U given a value of Z .

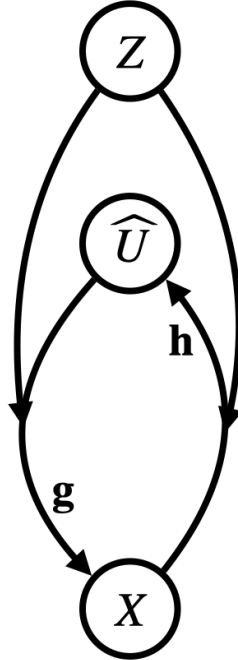


Figure 2: Structure in one node. Z is the parent of X , and our algorithm learns an encoder \mathbf{h} and a decoder \mathbf{g} so that the surrogate $\hat{U} = \mathbf{h}(Z, X)$ and $X = \mathbf{g}(Z, \hat{U})$.

We propose an encoder-decoder framework to recover the exogenous variable. Figure 2 gives the encoder-decoder structure in one node. With the observations of X and its parent Z , our method learns an encoder $\mathbf{h}()$ that aims to recover the value of U , i.e., $\hat{\mathbf{u}} = \mathbf{h}(\mathbf{z}, \mathbf{x})$; our algorithm also learns

a decoder $\mathbf{x} = \mathbf{g}(\mathbf{z}, \hat{\mathbf{u}})$ that provides us a surrogate model for $\mathbf{f}()$. As mentioned above, \hat{U} denotes the recovered U using the learned encoder, $\mathbf{h}()$.

Theorem 4.1 shows that the surrogate values of the exogenous variable U can be recovered from the observations of node X under the *decomposable generation mechanism (DGM)* assumption for \mathbf{f} , i.e. $X = \mathbf{f}(Z, U) = \mathbf{f}_a(Z) + \mathbf{f}_b(Z)\mathbf{f}_c(U)$.

Theorem 4.1. *Let (Z, U, X, \mathbf{f}) be a τ -SCM. Let $\phi()$ be a regression model, $\phi() : \mathcal{Z} \rightarrow \mathcal{X}$, with mean $\mu_\phi()$ and variance $\sigma_\phi()$. We define an encoder $\mathbf{h}() : \mathcal{Z} \times \mathcal{X} \rightarrow \hat{\mathcal{U}}$ with $\hat{U} := \mathbf{h}(Z, X) := \frac{X - \mu_\phi(Z)}{\sigma_\phi(Z)}$, and a decoder $\mathbf{g}() : \mathcal{Z} \times \hat{\mathcal{U}} \rightarrow \mathcal{X}$ with $X = \mathbf{g}(Z, \hat{U})$. We assume that $\mathbf{f}()$ is differentiable and has a decomposable structure as $X = \mathbf{f}(Z, U) = \mathbf{f}_a(Z) + \mathbf{f}_b(Z)\mathbf{f}_c(U)$, and $\mathbf{f}_b(Z) \neq 0$. Then with a constant a , $\hat{U} = a(\mathbf{f}_c(U) - \mathbb{E}[\mathbf{f}_c(U)])$, $\mathbb{E}[\hat{U}] = 0$, and $\hat{U} \perp\!\!\!\perp Z$.*

Remark 4.1. *We use the distribution of $\hat{U} = \mathbf{s}(U) = \mathbf{h}(Z, X)$, i.e. $p(\hat{U})$, to represent $p(U)$ in the surrogate model. With the decomposable assumption on $\mathbf{f}()$, a τ -SCM is counterfactually identifiable.*

DGM is significantly different from the ANM [12] mechanism given by $X = \mathbf{f}(\mathbf{pa}(X)) + U$, which is a linear monotonic function of U and widely used by many existing BO and CBO methods. In our DGM, $\mathbf{f}_c()$ can be any continuous function, including nonlinear, non-convex, and non-monotonic function classes regarding U . Moreover, $\mathbf{f}_b(Z)$ can be any continuous function as long as $\mathbf{f}_b(Z) \neq 0$. The last term of a DGM, i.e. $\mathbf{f}_b(Z)\mathbf{f}_c(U)$ indicates that given a fixed value of the parent Z , the generated variable X 's variance is not only determined by U but also by the value of Z . Therefore, with $\mathbf{f}_b(Z)$ DGM represents a larger class of mechanisms that both U and Z affect the variance of the generated variable X . These features substantially extend the identification of exogenous variable U to much broader nonlinear and non-monotonic data-generation mechanism classes compared to ANM (linear) and BGM (monotonic). In the surrogate model, $\mathbf{f}()$ is approximated with the learned $\mathbf{g}()$ and $\mathbf{s}()$, i.e., $\mathbf{x} = \mathbf{f}(\mathbf{z}, \mathbf{u}) = \mathbf{g}(\mathbf{z}, \hat{\mathbf{u}}) = \mathbf{g}(\mathbf{z}, \mathbf{s}(\mathbf{u}))$.

With the monotonic assumption on $\mathbf{f}()$, we are able to extend the encoder-decoder framework to BGMs by following [15; 17; 18; 8].

Theorem 4.2. *Let (Z, U, X, \mathbf{f}) be a τ -SCM. $\forall \mathbf{z} \in \mathcal{Z}$, $\mathbf{f}(\mathbf{z}, \cdot)$ is differentiable and strictly monotonic regarding $\mathbf{u} \in \mathcal{U}$. We define a differentiable and invertible encoder function $\mathbf{h}() : \mathcal{Z} \times \mathcal{X} \rightarrow \hat{\mathcal{U}}$, i.e., $\hat{U} := \mathbf{h}(Z, X)$, and $\hat{U} \perp\!\!\!\perp Z$. The decoder is $\mathbf{g}() : \mathcal{Z} \times \hat{\mathcal{U}} \rightarrow \mathcal{X}$, i.e., $X = \mathbf{g}(Z, \hat{U})$. Then $\hat{U} = \mathbf{h}(Z, X)$ is a function of U , i.e., $\hat{U} = \mathbf{s}(U)$, and $\mathbf{s}()$ is an invertible function.*

The proposed exogenous variable surrogate \hat{U} and encoder function, $\hat{U} = \mathbf{h}(Z, X) = \frac{X - \mu_\phi(Z)}{\sigma_\phi(Z)}$, work under either the decomposable generation mechanism (DGM) conditions in Theorem 4.1 or the bijective generation mechanism (BGM, [17]) in Theorem 4.2. This means our method is suitable for ANMs, DGMs, and BGMs. The proofs of Theorem 4.1 and Theorem 4.2 can be found in the Appendix.

For a BGM model, we need to enforce independence between \hat{U} and Z to recover U according to Theorem 4.2. It could be achieved by adding an independence regularization on both variables, which may introduce additional computation costs.

If $\mathbf{f}()$ doesn't meet the DGM and the BGM assumptions, the learned $\hat{U} = \frac{X - \mu_\phi(Z)}{\sigma_\phi(Z)}$ will not be independent of the parent variable Z , and we will not get an accurate surrogate model for the SCM, and it may decrease the possibility to attain the optimal objective value of y using limited training samples.

4.2 Implementation of Exogenous Distribution Learning

There are multiple ways to implement the encoder-decoder framework in Figure 2, e.g., via Variational Auto-Encoder (VAE) [13]. To make the implementation simple, we implement both the encoder and decoder using Gaussian Process regression models based on the result of Theorem 4.1 and Theorem 4.2. For a node with an action variable A , the decoder becomes $\mathbf{g}() : \mathcal{Z} \times \mathcal{A} \times \widehat{\mathcal{U}} \rightarrow \mathcal{X}$, the encoder becomes $\mathbf{h}() : \mathcal{Z} \times \mathcal{A} \times \mathcal{X} \rightarrow \widehat{\mathcal{U}}$, and $\phi() : \mathcal{Z} \times \mathcal{A} \rightarrow \mathcal{X}$. $\mathbf{g}()$ and $\phi()$ are implemented with Gaussian Process regression models.

We use a Gaussian Mixture model to fit the recovered distribution of $\widehat{\mathcal{U}}$, i.e. $p(\widehat{\mathcal{U}})$. We use $p(\widehat{\mathcal{U}})$ to replace $p(\mathcal{U})$ in the computing of the probabilistic surrogate objective. For the nodes in SCM \mathcal{M} , let $\mathbf{G} = \{\mathbf{g}_i\}_{i=0}^d$, and $\mathbf{H} = \{\mathbf{h}_i\}_{i=0}^d$.

5 CBO with Exogenous Distribution Learning

In this section, we present the EXCBO algorithm, describing the probabilistic model and acquisition function used.

5.1 Statistical Model

In our model, the function \mathbf{f}_i that generates variable X_i is learned through \mathbf{g}_i , and $X_i = \mathbf{g}_i(Z_i, A_i, \widehat{U}_i)$. We use Gaussian Processes [24] to learn the surrogate of \mathbf{g}_i , i.e., $\tilde{\mathbf{g}}_i$. For $i \in [d]$, let $\boldsymbol{\mu}_{g,i,0}$ and $\boldsymbol{\sigma}_{g,i,0}$ denote the prior mean and variance function for each \mathbf{f}_i , respectively.

Following [9], at time t , let $\tilde{\mathbf{G}}$ be the statistically plausible function set of \mathbf{G} , i.e., $\tilde{\mathbf{G}} = \{\tilde{\mathbf{g}}_i\}_{i=0}^d$. Similarly, the plausible model of \mathbf{H} is denoted $\tilde{\mathbf{H}} = \{\tilde{\mathbf{h}}_i\}_{i=0}^d$. Moreover, at step t , the observation set is $\mathcal{D}_t = \{\mathbf{z}_{:,1:t}, \mathbf{a}_{:,1:t}, \mathbf{x}_{:,1:t}\}$. The posterior of \mathbf{g}_i with the input of node i , $(\tilde{\mathbf{z}}_i, \tilde{\mathbf{a}}_i, \tilde{\mathbf{u}}_i)$, is given by

$$\begin{aligned} \tilde{\mathbf{g}}_{i,t}(\tilde{\mathbf{z}}_i, \tilde{\mathbf{a}}_i, \tilde{\mathbf{u}}_i) &\sim \mathcal{GP}(\boldsymbol{\mu}_{g,i,t-1}, \boldsymbol{\sigma}_{g,i,t-1}), \\ \boldsymbol{\mu}_{g,i,t-1} &= \boldsymbol{\mu}_{g,i,t-1}(\tilde{\mathbf{z}}_i, \tilde{\mathbf{a}}_i, \tilde{\mathbf{u}}_i), \\ \boldsymbol{\sigma}_{g,i,t-1} &= \boldsymbol{\sigma}_{g,i,t-1}(\tilde{\mathbf{z}}_i, \tilde{\mathbf{a}}_i, \tilde{\mathbf{u}}_i). \end{aligned}$$

Then $\tilde{\mathbf{x}}_{i,t} = \tilde{\mathbf{g}}_{i,t}(\tilde{\mathbf{z}}_i, \tilde{\mathbf{a}}_i, \tilde{\mathbf{u}}_i)$ denotes observations from one of the plausible models. Here $\tilde{\mathbf{u}}_i \sim p(\widehat{U}_i)$ in the sampling of the learned distribution of \widehat{U}_i .

Given an observation $(\mathbf{z}_i, \mathbf{a}_i, \mathbf{x}_i)$ at node i , the exogenous recovery $\hat{\mathbf{u}}_i = \mathbf{h}_i(\mathbf{z}_i, \mathbf{a}_i, \mathbf{x}_i) = \frac{\mathbf{x}_i - \boldsymbol{\mu}_{\phi,i}(\mathbf{z}_i, \mathbf{a}_i)}{\boldsymbol{\sigma}_{\phi,i}(\mathbf{z}_i, \mathbf{a}_i)}$. At time step t , the posterior of ϕ_i with the input of node i , $(\mathbf{z}_i, \mathbf{a}_i)$, is given by

$$\tilde{\phi}_{i,t}(\mathbf{z}_i, \mathbf{a}_i) \sim \mathcal{GP}(\boldsymbol{\mu}_{\phi,i,t-1}(\mathbf{z}_i, \mathbf{a}_i), \boldsymbol{\sigma}_{\phi,i,t-1}(\mathbf{z}_i, \mathbf{a}_i)) \quad (7)$$

Therefore, $\tilde{\mathbf{u}}_i = \tilde{\mathbf{h}}_{i,t}(\mathbf{z}_i, \mathbf{a}_i, \mathbf{x}_i) = \frac{\mathbf{x}_i - \boldsymbol{\mu}_{\phi,i,t-1}(\mathbf{z}_i, \mathbf{a}_i)}{\boldsymbol{\sigma}_{\phi,i,t-1}(\mathbf{z}_i, \mathbf{a}_i)}$. According to the definition of $\mathbf{h}()$ in Theorem 4.1, $\mathbf{h}()$ also follows a Gaussian Process, i.e.

$$\mathbf{h}_{i,t}(\mathbf{z}_i, \mathbf{a}_i, \mathbf{x}_i) \sim \mathcal{GP}(\boldsymbol{\mu}_{h,i,t-1}, \boldsymbol{\sigma}_{h,i,t-1}).$$

This GP is defined by $\tilde{\phi}_{i,t}()$ which is sampled with (7). Different from $\mathbf{g}_i()$, the observations of the input (Z_i, A_i, X_i) for $\mathbf{h}_i()$ are only required at the training time, and we only need to sample the learned $p(\widehat{U}_i)$ to get value $\hat{\mathbf{u}}_i$ for model prediction or model sampling.

5.2 Acquisition Function

Algorithm 1 describes the proposed method solving (6). In iteration t , it uses GP posterior belief of y to construct an upper confidence bound (UCB) [7] of y :

$$\text{UCB}_{t-1}(\mathbf{a}) = \boldsymbol{\mu}_{t-1}(\mathbf{a}) + \beta_t \boldsymbol{\sigma}_{t-1}(\mathbf{a}). \quad (8)$$

Here

$$\begin{aligned} \boldsymbol{\mu}_{t-1}(\mathbf{a}) &= \mathbb{E}[\boldsymbol{\mu}_{g,d,t-1}(\tilde{\mathbf{z}}_d, \tilde{\mathbf{a}}_d, \tilde{\mathbf{u}}_d)], \\ \boldsymbol{\sigma}_{t-1}(\mathbf{a}) &= \mathbb{E}[\boldsymbol{\sigma}_{g,d,t-1}(\tilde{\mathbf{z}}_d, \tilde{\mathbf{a}}_d, \tilde{\mathbf{u}}_d)], \end{aligned}$$

where the expectation is taken over $p(\widehat{U})$. In (8), β_t controls the tradeoff between exploration and exploitation of Algorithm 1. The UCB-based algorithm is a classic strategy that is widely used in BO and stochastic bandits [14; 22]. The proposed algorithm adapts the ‘‘optimism in the face of uncertainty’’ (OFU) strategy by taking the expectation of the UCB as part of the acquisition process.

5.3 Algorithm

Let $k_{g,i}, k_{\phi,i}, \forall i \in [d]$ represent the kernel functions of \mathbf{g}_i and ϕ_i . The proposed EXCBO algorithm is summarized by Algorithm 1. In each iteration, a new sample is observed according to the UCB values. Then the posteriors of \mathbf{G} and \mathbf{H} are updated with the new dataset. The next section gives a theoretical analysis of the algorithm.

Algorithm 1 EXCBO

Input: $k_{g,i}, k_{\phi,i}, \forall i \in [d]$

Result: Intervention actions $\mathbf{a}_i, \forall i \in [d]$

for $t = 1$ **to** T **do**

Find \mathbf{a}_t by optimizing the acquisition function, $\mathbf{a}_t \in \arg \max \text{UCB}_{t-1}(\mathbf{a})$;

Observe samples $\{\mathbf{z}_{i,t}, \mathbf{x}_{i,t}\}_{i=0}^d$ with \mathbf{a}_t and update \mathcal{D}_t ;

Use \mathcal{D}_t to update posteriors $\{\boldsymbol{\mu}_{\phi,i,t}, \boldsymbol{\sigma}_{\phi,i,t}^2\}_{i=0}^d$ and sample $\{\hat{\mathbf{u}}_{i,t}\}_{i=0}^d$;

Use $\mathcal{D}_t \cup \{\hat{\mathbf{u}}_{i,t}\}_{i=0}^d$ to update posteriors $\{\boldsymbol{\mu}_{g,i,t}, \boldsymbol{\sigma}_{g,i,t}^2\}_{i=0}^d$;

end for

6 Theoretical Study

This section describes the convergence guarantees for EXCBO using soft interventions. Our analysis follows the theoretical study in [23] and shows that EXCBO has a sublinear cumulative regret bound. We first introduce additional technical assumptions used in the analysis.

Assumption 6.1 gives the Lipschitz conditions of $\mathbf{g}_i, \boldsymbol{\sigma}_{g,i}$, and $\boldsymbol{\mu}_{g,i}$. It holds if the RKHS of each \mathbf{g}_i has a Lipschitz continuous kernel [10; 23]. Assumption 6.3 holds when we assume that the i th GP prior uses the same kernel as the RKHS of \mathbf{g}_i and that $\beta_{i,t}$ is sufficiently large to ensure the confidence bounds in

$$\begin{aligned} & \left| \mathbf{g}_i(\mathbf{z}_i, \mathbf{a}_i, \hat{\mathbf{u}}_i) - \boldsymbol{\mu}_{g,i,t-1}(\mathbf{z}_i, \mathbf{a}_i, \hat{\mathbf{u}}_i) \right| \\ & \leq \beta_{i,t} \boldsymbol{\sigma}_{g,i,t-1}(\mathbf{z}_i, \mathbf{a}_i, \hat{\mathbf{u}}_i) \quad \forall \mathbf{z}_i \in \mathcal{Z}_i, \mathbf{a}_i \in \mathcal{A}_i, \hat{\mathbf{u}}_i \in \widehat{\mathcal{U}}_i. \end{aligned}$$

Assumption 6.1. $\forall \mathbf{g}_i \in \mathbf{G}$, \mathbf{g}_i is $L_{\mathbf{g}}$ -Lipschitz continuous; moreover, $\forall i, t$, $\boldsymbol{\mu}_{g,i,t}$ and $\boldsymbol{\sigma}_{g,i,t}$ are $L_{\boldsymbol{\mu}_g}$ and $L_{\boldsymbol{\sigma}_g}$ Lipschitz continuous.

Assumption 6.2. $\forall \mathbf{f}_i \in \mathbf{F}$, \mathbf{f}_i is differentiable and has a decomposable structure with $X = \mathbf{f}_i(Z_i, U_i) = \mathbf{f}_{i(a)}(Z_i) + \mathbf{f}_{i(b)}(Z_i)\mathbf{f}_{i(c)}(U_i)$, and $\mathbf{f}_{i(b)}(\mathbf{z}_i) \neq 0, \forall \mathbf{z}_i \in \mathcal{Z}_i$.

Assumption 6.3. $\forall i, t$, there exists sequence $\beta_{i,t} \in \mathbb{R}_{>0}$, with probability at least $(1 - \alpha)$, for all $\mathbf{z}_i, \mathbf{a}_i, \hat{\mathbf{u}}_i \in \mathcal{Z}_i \times \mathcal{A}_i \times \hat{\mathcal{U}}_i$ we have $|\mathbf{g}_i(\mathbf{z}_i, \mathbf{a}_i, \hat{\mathbf{u}}_i) - \boldsymbol{\mu}_{g,i,t-1}(\mathbf{z}_i, \mathbf{a}_i, \hat{\mathbf{u}}_i)| \leq \beta_{i,t}\boldsymbol{\sigma}_{g,i,t-1}(\mathbf{z}_i, \mathbf{a}_i, \hat{\mathbf{u}}_i)$, and $|\mathbf{h}(\mathbf{z}_i, \mathbf{a}_i, \mathbf{x}_i) - \boldsymbol{\mu}_{h,i,t-1}(\mathbf{z}_i, \mathbf{a}_i, \mathbf{x}_i)| \leq \beta_{i,t}\boldsymbol{\sigma}_{h,i,t-1}(\mathbf{z}_i, \mathbf{a}_i, \mathbf{x}_i)$.

In the DAG \mathcal{G} over $\{X_i\}_0^d$, let N be the maximum distance from a root to X_d , i.e., $N = \max_i \text{dist}(X_i, X_d)$. Here $\text{dist}(\cdot, \cdot)$ is a measure of the edges in the longest path from X_i to the reward node X_d . Let M denote the maximum number of parents of any variables in \mathcal{G} , $M = \max_i |\mathbf{pa}(i)|$. Let L_t be a function of $L_{\mathbf{g}}$, $L_{\boldsymbol{\sigma}_g}$, and N . The following theorem bounds the performance of EXCBO in terms of cumulative regret.

Theorem 6.1. Consider the optimization problem in (6), with the SCM satisfying Assumptions 6.1-6.3, where \mathcal{G} is known but \mathbf{F} is unknown. Then with probability at least $1 - \alpha$, the cumulative regret of Algorithm 1 is bounded by

$$R_T \leq \mathcal{O}(L_T M^N d \sqrt{T \gamma_T}).$$

Here $\gamma_T = \max_t \gamma_{i,T}$ denote the maximum information gain at time T . This maximum information gain is commonly used in many Bayesian Optimizations [22]. Many common kernels, such as linear and squared exponential kernels, lead to sublinear information gain in T , and it results in an overall sublinear regret for EXCBO [23]. The proof of Theorem 6.1 and further analysis can be found in the Appendix.

The analysis focuses on the DGM mechanisms. To extend the analysis to BGMs, we need to consider the computation cost involving the independence penalization on variables \hat{U} and Z . For mechanisms beyond DGMs and BGMs, we conjecture that the surrogate approximation accuracy may decrease, but the convergence rate may not decrease a lot. We leave the regret analysis beyond DGMs to future works.

7 Experimental Study

This section presents experimental comparisons of the proposed EXCBO and existing algorithms.

7.1 Baselines

We compare EXCBO against three algorithms: UCB, EICF, and MCBO, where UCB is a conventional method of BO [7]; EICF [3] is the composite function method of BO; MCBO [23] is the CBO method discussed in previous sections. Different from the other methods, MCBO relies on neural networks along with the GPs to model the uncertainty. All algorithms are implemented with Python and BoTorch [6], and we use the implementations of UCB, EICF, and MCBO in the package published with [23]. The initial observation size for MCBO is the default value from the package [23], which is $2(|A| + 1)$, and $|A|$ is the number of action variables. For other methods, the initial sample size is in the range of [5, 20]. We use four different random seeds to run all the algorithms to obtain the means and standard derivations of the reward values.

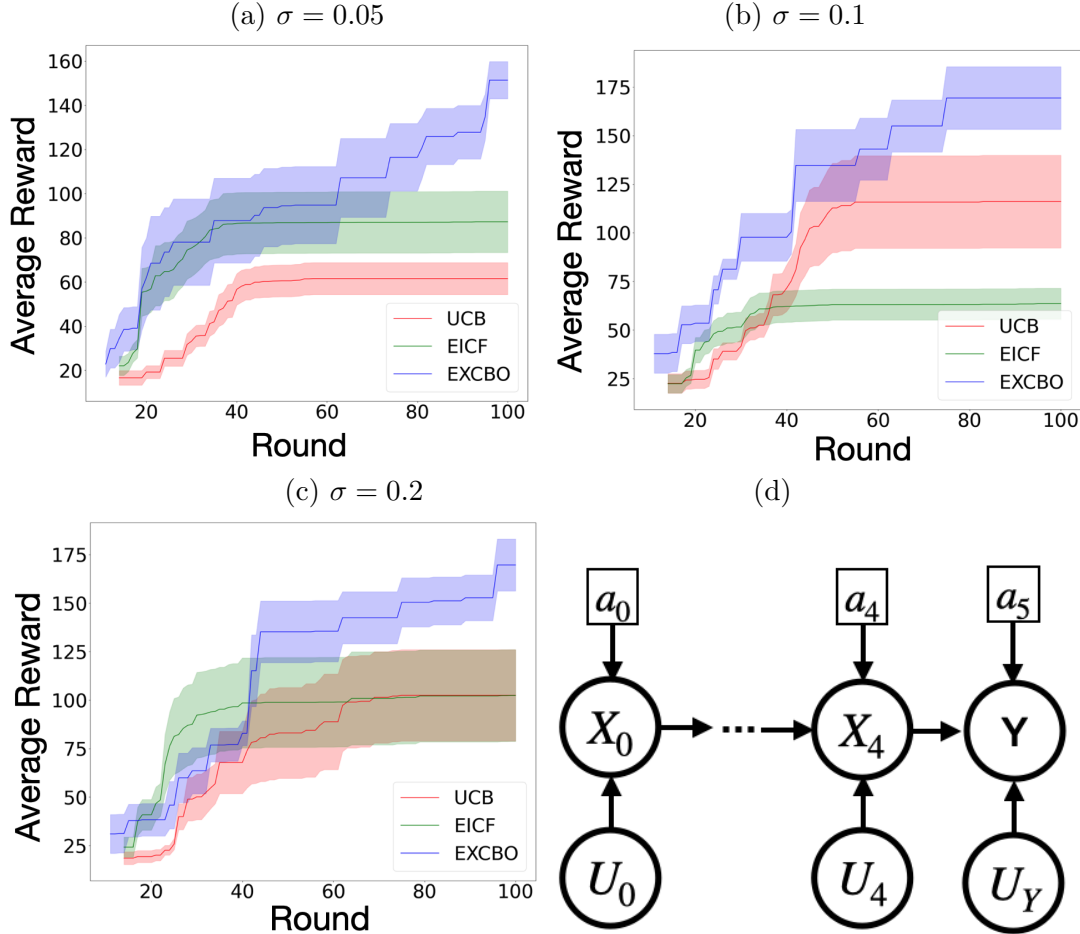


Figure 3: (a-c): results of Alpine2 at different noise levels; (d): Alpine2 graph structure.

7.2 Alpine2 Dataset

We study the algorithms using the Alpine2 dataset. There are six endogenous nodes in the Alpine2 dataset as shown in Figure 3-(d). The exogenous distributions for X and Y are Gaussian Mixture models with two components, i.e.,

$$\begin{aligned}
 p(U) &= w_1 \mathcal{N}(\mu_1, c_1 \sigma) + w_2 \mathcal{N}(\mu_2, c_2 \sigma), \\
 w_1, w_2, c_1, c_2 &> 0.
 \end{aligned} \tag{9}$$

Due to the excessively long computing time used by MCBO, we have only two baselines in this set of experiments, i.e., UCB and EICF. The results of Alpine2 are shown in Figures 3-(a-c). As shown in the plots, our EXCBO performs the best on all three noise levels. It proves the effectiveness and benefits of the proposed EXCBO method.

7.3 Epidemic Model Calibration

We test EXCBO on an epidemic model calibration by following the setup in [4]. In this model as shown in Figure 4, $I_{i,t}$ represents the fraction of the population in group i that are “infectious” at time t ; $\beta_{i,j,t}$ is the rate of the people from group i who are “susceptible” have close physical contact with people in group j who are “infectious” at time t . We assume there are two groups, and

infections resolve at a rate of γ per period. The number of infectious individuals in group i at the start of the next time period is $I_{i,t+1} = I_{i,t}(1 - \gamma) + (1 - I_{i,t}) \sum_j \beta_{i,j,t} I_{j,t}$. We assume each $I_{i,t}$ has an observation noise $U_{i,t}$. The model calibration problem is that given limited noisy observations of $I_{i,t}$ s, how to efficiently find the $\beta_{i,j,t}$ values in the model. The reward is defined as the negative mean square error (MSE) of all the $I_{i,t}$ observations as the objective function to optimize. In this model, $\beta_{i,j,t}$ s are the action variables.

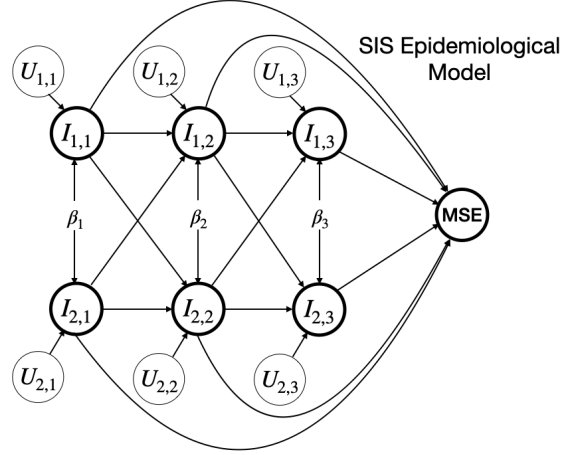


Figure 4: Graph structure for epidemic model calibration.

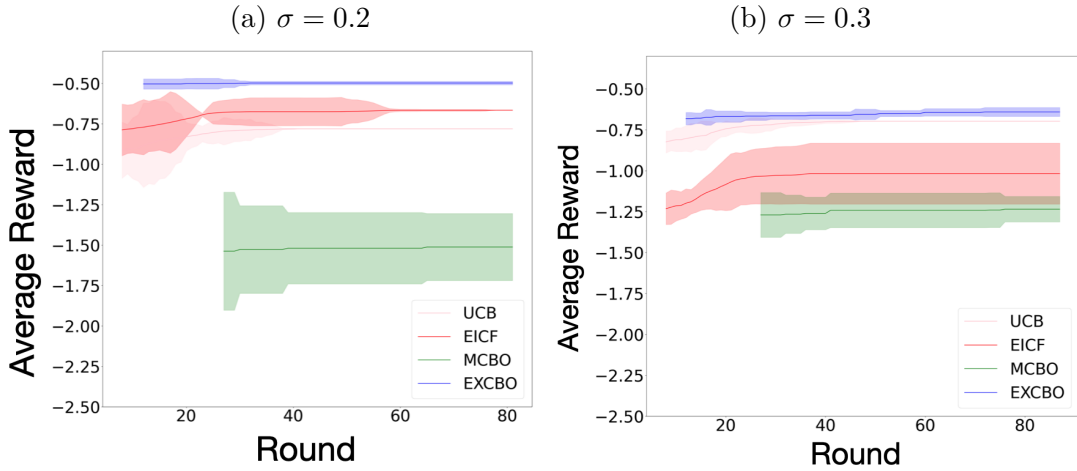


Figure 5: Results of epidemic model calibration.

Figure 5 visualizes the results at the noise levels with $\sigma = 0.2$ and $\sigma = 0.3$. The noise is added with two models as in (9). As shown in Figure 5, our EXCBO always performs better than state-of-the-art model calibration methods in both cases, and our method has a faster convergence rate compared to the baselines. With the capability to recover and learn the noise distributions, our method is more robust and stable in this application scenario.

7.4 Pooled Testing for COVID-19

We further compare EXCBO and existing methods using the COVID-19 pooled testing problem [4]. The graphical structure is given by Figure 6. In Figure 6, I_t is the fraction of the population that is

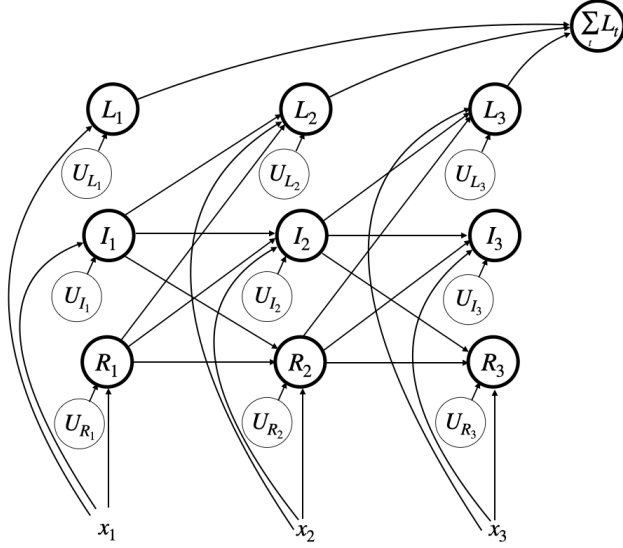


Figure 6: Graph structure for COVID-19 pooled testing problem.

infectious at time t ; R_t is the fraction of the population that is recovered and cannot be infected again, and time point $t \in \{1, 2, 3\}$. The additional fraction $S_t = 1 - I_t - R_t$ of the population is susceptible and can be infected. During each period t , the entire population is tested using a pool size of x_t . The loss L_t , incorporates the costs resulting from infections, testing resources used, and individuals isolated at period t . The objective is to choose pool size x_t to minimize the total loss $\sum_t L_t$. Therefore, x_t s are the action variables/nodes that the algorithms try to optimize to achieve lower costs. Figure 7 gives the optimization results from different methods, where the reward $y = -\sum_t L_t$. The proposed method EXCBO achieves the best rewards at both noise levels $\sigma = 0.2$ and $\sigma = 0.4$. MCBO's inferior results on this dataset might be because of the over-fitting issue of the neural networks.

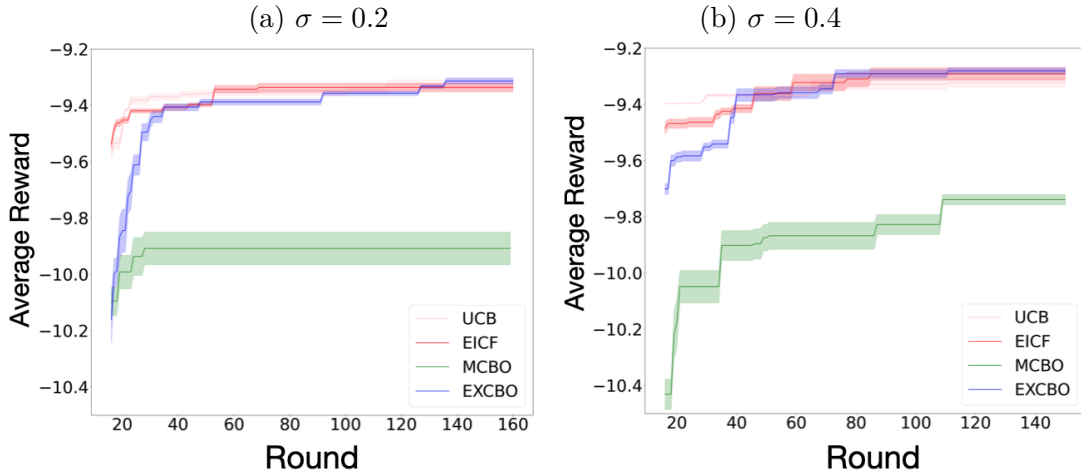


Figure 7: Results of COVID-19 pooled testing optimization.

8 Conclusions

We propose a novel Causal Bayesian Optimization method, EXCBO, that approximately recovers the endogenous variables in a structured causal model. With the recovered exogenous distribution, our method naturally improves the surrogate model’s accuracy in the approximation of SCMs. Furthermore, the recovered exogenous variables may enhance the surrogate model’s capability in causal inference and hence improve the sample efficiency of CBO. We additionally provide theoretical analysis on both exogenous variable recovery and the algorithm’s cumulative regret bound. Experiments on multiple datasets show the algorithm’s soundness and benefits.

References

- [1] Virginia Aglietti, Neil Dhir, Javier González, and Theodoros Damoulas. Dynamic causal bayesian optimization. *Advances in Neural Information Processing Systems*, 34:10549–10560, 2021.
- [2] Virginia Aglietti, Xiaoyu Lu, Andrei Paleyes, and Javier González. Causal bayesian optimization. In *International Conference on Artificial Intelligence and Statistics*, pages 3155–3164. PMLR, 2020.
- [3] Raul Astudillo and Peter Frazier. Bayesian optimization of composite functions. In *International Conference on Machine Learning*, pages 354–363. PMLR, 2019.
- [4] Raul Astudillo and Peter Frazier. Bayesian optimization of function networks. *Advances in neural information processing systems*, 34:14463–14475, 2021.
- [5] Raul Astudillo and Peter I Frazier. Thinking inside the box: A tutorial on grey-box bayesian optimization. In *2021 Winter Simulation Conference (WSC)*, pages 1–15. IEEE, 2021.
- [6] Maximilian Balandat, Brian Karrer, Daniel R. Jiang, Samuel Daulton, Benjamin Letham, Andrew Gordon Wilson, and Eytan Bakshy. BoTorch: A Framework for Efficient Monte-Carlo Bayesian Optimization. In *Advances in Neural Information Processing Systems 33*, 2020.
- [7] Eric Brochu, Vlad M Cora, and Nando De Freitas. A tutorial on bayesian optimization of expensive cost functions, with application to active user modeling and hierarchical reinforcement learning. *arXiv preprint arXiv:1012.2599*, 2010.
- [8] Patrick Chao, Patrick Blöbaum, and Shiva Prasad Kasiviswanathan. Interventional and counterfactual inference with diffusion models. *ArXiv*, abs/2302.00860, 2023.
- [9] Sayak Ray Chowdhury and Aditya Gopalan. Online learning in kernelized markov decision processes. In *The 22nd International Conference on Artificial Intelligence and Statistics*, pages 3197–3205. PMLR, 2019.
- [10] Sebastian Curi, Felix Berkenkamp, and Andreas Krause. Efficient model-based reinforcement learning through optimistic policy search and planning. *Advances in Neural Information Processing Systems*, 33:14156–14170, 2020.
- [11] Clark Glymour, Kun Zhang, and Peter Spirtes. Review of causal discovery methods based on graphical models. *Frontiers in genetics*, 10:524, 2019.

- [12] Patrik Hoyer, Dominik Janzing, Joris M Mooij, Jonas Peters, and Bernhard Schölkopf. Nonlinear causal discovery with additive noise models. *Advances in neural information processing systems*, 21, 2008.
- [13] Diederik P Kingma and Max Welling. Auto-encoding variational bayes. *arXiv preprint arXiv:1312.6114*, 2013.
- [14] Tor Lattimore and Csaba Szepesvári. *Bandit algorithms*. Cambridge University Press, 2020.
- [15] C. Lu, B. Huang, K. Wang, J. M. Hernández-Lobato, K. Zhang, and B. Schölkopf. Sample-efficient reinforcement learning via counterfactual-based data augmentation. In *Offline Reinforcement Learning - Workshop at the 34th Conference on Neural Information Processing Systems (NeurIPS)*, 2020.
- [16] Jonas Moćkus. On bayesian methods for seeking the extremum. In *Optimization Techniques IFIP Technical Conference: Novosibirsk, July 1–7, 1974*, pages 400–404. Springer, 1975.
- [17] Arash Nasr-Esfahany, Mohammad Alizadeh, and Devavrat Shah. Counterfactual identifiability of bijective causal models. *arXiv preprint arXiv:2302.02228*, 2023.
- [18] Arash Nasr-Esfahany and Emre Kiciman. Counterfactual (non-)identifiability of learned structural causal models. *arXiv preprint arXiv:2301.09031*, 2023.
- [19] Leland Gerson Neuberger. Causality: models, reasoning, and inference, by judea pearl, cambridge university press, 2000. *Econometric Theory*, 19(4):675–685, 2003.
- [20] Judea Pearl. Causal diagrams for empirical research. *Biometrika*, 82(4):669–688, 1995.
- [21] Jonas Peters, Dominik Janzing, and Bernhard Schölkopf. *Elements of causal inference: foundations and learning algorithms*. The MIT Press, 2017.
- [22] Niranjan Srinivas, Andreas Krause, Sham M Kakade, and Matthias Seeger. Gaussian process optimization in the bandit setting: No regret and experimental design. *arXiv preprint arXiv:0912.3995*, 2009.
- [23] Scott Sussex, Anastasiia Makarova, and Andreas Krause. Model-based causal bayesian optimization. *arXiv preprint arXiv:2211.10257*, 2022.
- [24] Christopher KI Williams and Carl Edward Rasmussen. *Gaussian processes for machine learning*. MIT press Cambridge, MA, 2006.

Supplementary Material for ‘Causal Bayesian Optimization via
Exogenous Distribution Learning’

A Analysis on Exogenous Variable Recovery

A.1 Proof of Theorem 4.1

Before we prove Theorem 4.1, we present a similar result for ANMs.

Theorem A.1. *Let (X, Z, U, \mathbf{f}) be a τ -SCM. Let $\boldsymbol{\rho}() : \mathcal{X} \times \mathcal{Z} \rightarrow \mathbb{R}^1$ be a predefined function regarding X and Z , and $\phi()$ be a regression model with $\phi() : \mathcal{Z} \rightarrow \boldsymbol{\rho}(\mathcal{X}, \mathcal{Z})$. We define an encoder function $\mathbf{h}() : \mathcal{Z} \times \mathcal{X} \rightarrow \hat{U}$ with $\hat{U} := \mathbf{h}(Z, X) := \boldsymbol{\rho}(X, Z) - \phi(Z)$. The decoder is $\mathbf{g}() : \mathcal{Z} \times \hat{U} \rightarrow \mathcal{X}$, i.e., $X = \mathbf{g}(Z, \hat{U})$. Let $\boldsymbol{\rho}()$ maps the values of X and Z to an additive function of Z and U , i.e., $\boldsymbol{\rho}(X, Z) = \boldsymbol{\rho}_1(Z) + \boldsymbol{\rho}_2(U)$. Then $\hat{U} = \mathbf{h}(Z, X) = \boldsymbol{\rho}_2(U) - \mathbb{E}[\boldsymbol{\rho}_2(U)]$, and $\hat{U} \perp\!\!\!\perp Z$.*

Proof. As $\phi(\mathbf{z})$ is an optimal approximation of $\boldsymbol{\rho}(X, \mathbf{z})$, with $Z \perp\!\!\!\perp U$, we have

$$\begin{aligned} \phi(\mathbf{z}) &= \mathbb{E}[\boldsymbol{\rho}(X, \mathbf{z})] = \mathbb{E}[\boldsymbol{\rho}_1(\mathbf{z}) + \boldsymbol{\rho}_2(U)] = \int (\boldsymbol{\rho}_1(\mathbf{z}) + \boldsymbol{\rho}_2(\mathbf{u}))p(\mathbf{u})d\mathbf{u} \\ &= \boldsymbol{\rho}_1(\mathbf{z}) + \mathbb{E}[\boldsymbol{\rho}_2(U)]. \end{aligned}$$

Thus, the decoder becomes

$$\begin{aligned} \mathbf{h}(\mathbf{z}, \mathbf{x}) &= \boldsymbol{\rho}(\mathbf{x}, \mathbf{z}) - \phi(Z = \mathbf{z}) \\ &= \boldsymbol{\rho}_1(\mathbf{z}) + \boldsymbol{\rho}_2(\mathbf{u}) - \boldsymbol{\rho}_1(\mathbf{z}) - \mathbb{E}[\boldsymbol{\rho}_2(U)] \\ &= \boldsymbol{\rho}_2(\mathbf{u}) - \mathbb{E}[\boldsymbol{\rho}_2(U)]. \end{aligned}$$

Therefore, $\hat{U} = \mathbf{h}(Z, X) = \boldsymbol{\rho}_2(U) - \mathbb{E}[\boldsymbol{\rho}_2(U)]$ is a function of U , and $\mathbf{h}(Z, X) \perp\!\!\!\perp Z$, i.e., $\hat{U} \perp\!\!\!\perp Z$. \square

Example A.1. *For an ANM model $X = f(Z) + U$, we have $\boldsymbol{\rho}(X, Z) = X$, $\boldsymbol{\rho}_1(Z) = f(Z)$, and $\boldsymbol{\rho}_2(U) = U$, then $\hat{U} = \mathbf{h}(Z, X) = U - \bar{U}$.*

Example A.2. *For a model $X = 2Ze^{-U} - e^{-Z}$, we have $\boldsymbol{\rho}(X, Z) = \log(X + e^{-Z})$, $\boldsymbol{\rho}_1(Z) = \log(2Z)$, and $\boldsymbol{\rho}_2(U) = -U$, then $\hat{U} = \mathbf{h}(Z, X) = -U + \bar{U}$.*

Example A.1 shows that the exogenous variable in any ANM model is identifiable. In practice, variable X 's generation mechanism $\mathbf{f}()$ is generally unknown, and it is hard to propose a general form function $\boldsymbol{\rho}()$ that can perform on any $\mathbf{f}()$ s and transform them to ANMs.

Theorem 4.1 *Let (Z, U, X, \mathbf{f}) be a τ -SCM. Let $\phi()$ be a regression model, $\phi() : \mathcal{Z} \rightarrow \mathcal{X}$, with mean $\boldsymbol{\mu}_\phi()$ and variance $\boldsymbol{\sigma}_\phi()$. We define an encoder $\mathbf{h}() : \mathcal{Z} \times \mathcal{X} \rightarrow \hat{U}$ with $\hat{U} := \mathbf{h}(Z, X) := \frac{X - \boldsymbol{\mu}_\phi(Z)}{\boldsymbol{\sigma}_\phi(Z)}$, and a decoder $\mathbf{g}() : \mathcal{Z} \times \hat{U} \rightarrow \mathcal{X}$ with $X = \mathbf{g}(Z, \hat{U})$. We assume that $\mathbf{f}()$ is differentiable and has a decomposable structure as $X = \mathbf{f}(Z, U) = \mathbf{f}_a(Z) + \mathbf{f}_b(Z)\mathbf{f}_c(U)$, and $\mathbf{f}_b(Z) \neq 0$. Then with a constant a , $\hat{U} = a(\mathbf{f}_c(U) - \mathbb{E}[\mathbf{f}_c(U)])$, $\mathbb{E}[\hat{U}] = 0$, and $\hat{U} \perp\!\!\!\perp Z$.*

Proof. As $\phi(\mathbf{z})$ is an optimal approximation of any value of $X = \mathbf{f}(\mathbf{z}, U)$, with $Z \perp\!\!\!\perp U$, we have the mean function as

$$\begin{aligned} \boldsymbol{\mu}_\phi(\mathbf{z}) &= \mathbb{E}[X(\mathbf{z}, U)] = \int (\mathbf{f}_a(\mathbf{z}) + \mathbf{f}_b(\mathbf{z})\mathbf{f}_c(\mathbf{u}))p(\mathbf{u})d\mathbf{u} \\ &= \mathbf{f}_a(\mathbf{z}) + \int \mathbf{f}_b(\mathbf{z})\mathbf{f}_c(\mathbf{u})p(\mathbf{u})d\mathbf{u} \\ &= \mathbf{f}_a(\mathbf{z}) + \mathbf{f}_b(\mathbf{z})\mathbb{E}[\mathbf{f}_c(U)]. \end{aligned}$$

Then with $U = \mathbf{u}$,

$$\begin{aligned}
& \mathbf{x} - \boldsymbol{\mu}_\phi(\mathbf{z}) \\
&= \mathbf{f}_a(\mathbf{z}) + \mathbf{f}_b(\mathbf{z})\mathbf{f}_c(\mathbf{u}) - \mathbf{f}_a(\mathbf{z}) - \mathbf{f}_b(\mathbf{z})\mathbb{E}[\mathbf{f}_c(U)] \\
&= \mathbf{f}_b(\mathbf{z})(\mathbf{f}_c(\mathbf{u}) - \mathbb{E}[\mathbf{f}_c(U)]).
\end{aligned} \tag{10}$$

With (10), the variance of regression model $\phi(\cdot)$ is

$$\begin{aligned}
& \mathbb{E}[(X - \boldsymbol{\mu}_\phi(\mathbf{z}))^2] \\
&= \mathbb{E}\left[\mathbf{f}_b(\mathbf{z})(\mathbf{f}_c(U) - \mathbb{E}[\mathbf{f}_c(U)])^2\mathbf{f}_b(\mathbf{z})\right] \\
&= \mathbf{f}_b^2(\mathbf{z})\mathbb{E}\left[(\mathbf{f}_c(U) - \mathbb{E}[\mathbf{f}_c(U)])^2\right] \\
&= \mathbf{f}_b^2(\mathbf{z})\boldsymbol{\sigma}_{\mathbf{f}_c}^2.
\end{aligned}$$

As $Z \perp\!\!\!\perp U$, as a function of Z , the learned variance $\boldsymbol{\sigma}_\phi^2(\mathbf{z})$ does not capture the information of U . $\boldsymbol{\sigma}_\phi^2(\mathbf{z})$ learns the variance function with respect to variable Z , i.e., $\mathbf{f}_2^2(\mathbf{z})$. Therefore, $\boldsymbol{\sigma}_\phi(\mathbf{z}) = c|\mathbf{f}_b(\mathbf{z})|$. Then, by (10),

$$\begin{aligned}
\frac{\mathbf{x} - \boldsymbol{\mu}_\phi(\mathbf{z})}{\boldsymbol{\sigma}_\phi(\mathbf{z})} &= \frac{\mathbf{f}_b(\mathbf{z})(\mathbf{f}_c(\mathbf{u}) - \mathbb{E}[\mathbf{f}_c(U)])}{c|\mathbf{f}_b(\mathbf{z})|} \\
&= \frac{s}{c}(\mathbf{f}_c(\mathbf{u}) - \mathbb{E}[\mathbf{f}_c(U)]).
\end{aligned} \tag{11}$$

Here $s = \text{sign}[\mathbf{f}_b(\mathbf{z})]$. Let $a = \frac{s}{c}$, we define

$$\widehat{U} := \frac{X - \boldsymbol{\mu}_\phi(Z)}{\boldsymbol{\sigma}_\phi(Z)} = a(\mathbf{f}_c(U) - \mathbb{E}[\mathbf{f}_c(U)]).$$

It shows that $\mathbb{E}[\widehat{U}] = 0$, and $\widehat{U} \perp\!\!\!\perp Z$. □

It is easy to show that a τ -SCM with a decomposable $\mathbf{f}(\cdot)$ is counterfactually identifiable. Hence, Theorem 4.1 presents a new family of τ -SCMs that are counterfactually identifiable beyond BGMs (Bijective Generation Mechanisms, [17]).

A.2 Proof of Theorem 4.2

In this section, we present the proof of Theorem 4.2, and the proof is based on the analysis in [17; 18; 15].

Theorem 4.2 *Let (Z, U, X, \mathbf{f}) be a τ -SCM. $\forall \mathbf{z} \in \mathcal{Z}$, $\mathbf{f}(\mathbf{z}, \cdot)$ is differentiable and strictly monotonic regarding $\mathbf{u} \in \mathcal{U}$. We define a differentiable and invertible encoder function $\mathbf{h}(\cdot) : \mathcal{Z} \times \mathcal{X} \rightarrow \widehat{\mathcal{U}}$, i.e., $\widehat{U} := \mathbf{h}(Z, X)$, and $\widehat{U} \perp\!\!\!\perp Z$. The decoder is $\mathbf{g}(\cdot) : \mathcal{Z} \times \widehat{\mathcal{U}} \rightarrow \mathcal{X}$, i.e., $X = \mathbf{g}(Z, \widehat{U})$. Then $\widehat{U} = \mathbf{h}(Z, X)$ is a function of U , i.e., $\widehat{U} = \mathbf{s}(U)$, and $\mathbf{s}(\cdot)$ is an invertible function.*

Proof. As U is the exogenous variable of endogenous node X , we have $X \perp\!\!\!\perp U$. According to Assumption-1, $\forall \mathbf{z} \in \mathcal{Z}$, $\mathbf{f}(\mathbf{z}, \mathbf{u})$ is differentiable and strictly monotonic regarding \mathbf{u} . Hence $X = \mathbf{f}(Z, U)$ is a BGM, and we use \mathbb{F} to represent BGM class that satisfies the independence ($X \perp\!\!\!\perp U$) and the function monotone conditions. We can see that $\mathbf{h}^{-1} \in \mathbb{F}$, $\mathbf{h}^{-1}(\cdot) = \mathbf{g}(\cdot)$, and \mathbf{h}^{-1} and \mathbf{f} are counterfactually equivalent BGMs that generate the same distribution $p(Z, X)$. Based Lemma B.2, Proposition 6.2, and Definition 6.1 in [17], there exists an invertible function $\mathbf{s}(\cdot)$ that satisfies $\forall \mathbf{z} \in \mathcal{Z}, \mathbf{x} \in \mathcal{X}, \mathbf{h}(\mathbf{z}, \mathbf{x}) = \mathbf{s}(\mathbf{f}^{-1}(\mathbf{z}, \mathbf{x}))$, i.e., $\widehat{\mathbf{u}} = \mathbf{s}(\mathbf{u})$, which is $\widehat{U} = \mathbf{s}(U)$. □

B Regret Analysis

Our analysis follows the study in [23]. In the DAG \mathcal{G} over $\{X_i\}_0^d$, let N be the maximum distance from a root to X_d , i.e., $N = \max_i \text{dist}(X_i, X_d)$. Here $\text{dist}(\cdot, \cdot)$ is a measure of the edges in the longest path from X_i to the reward node X_d . Let M denote the maximum number of parents of any variables in \mathcal{G} , $M = \max_i |\text{pa}(i)|$. Let L_t be a function of L_g, L_{σ_g} . According to Theorem 4.1, with the encoder-decoder structure given in Figure 2 in the main text, the exogenous variable and its distribution can be recovered. For each observation of the dynamic surrogate model, we assume the sampling of $p(\hat{U})$, $\hat{\mathbf{u}} = \mathbf{s}(\hat{\mathbf{u}}) = \mathbf{s}(\mathbf{u})$. The following lemma bounds the value of $\hat{\mathbf{u}}$ with the variance of the encoder.

Lemma B.1.

$$\|\hat{\mathbf{u}}_{i,t} - \tilde{\mathbf{u}}_{i,t}\| \leq 2\beta_t \|\sigma_{\hat{\mathbf{u}}_{i,t-1}}\| = 2\beta_t \|\sigma_{h,i,t-1}\|.$$

Proof. With Assumption 6.3 and $\hat{\mathbf{u}}_{i,t} = \mathbf{h}_{i,i-1}(\mathbf{z}_i, \mathbf{a}_i, \mathbf{x}_i)$, let $\tilde{\mathbf{u}}_{i,t} = \mu_{\hat{\mathbf{u}}_{i,t-1}}(\mathbf{z}_i, \mathbf{a}_i, \mathbf{x}_i) + \beta_t \sigma_{\hat{\mathbf{u}}_{i,t-1}}(\mathbf{z}_i, \mathbf{a}_i, \mathbf{x}_i) \circ \omega_{\hat{\mathbf{u}}_{i,t-1}}(\mathbf{z}_i, \mathbf{a}_i, \mathbf{x}_i)$, and here $|\omega_{\hat{\mathbf{u}}_{i,t-1}}(\mathbf{z}_i, \mathbf{a}_i, \mathbf{x}_i)| \leq 1$. Then

$$\begin{aligned} \|\hat{\mathbf{u}}_{i,t} - \tilde{\mathbf{u}}_{i,t}\| &= \|\tilde{\mathbf{u}}_{i,t} - \mu_{\hat{\mathbf{u}}_{i,t-1}}(\mathbf{z}_i, \mathbf{a}_i, \mathbf{x}_i) - \beta_t \sigma_{\hat{\mathbf{u}}_{i,t-1}}(\mathbf{z}_i, \mathbf{a}_i, \mathbf{x}_i) \circ \omega_{\hat{\mathbf{u}}_{i,t-1}}(\mathbf{z}_i, \mathbf{a}_i, \mathbf{x}_i)\| \\ &\leq \|\tilde{\mathbf{u}}_{i,t} - \mu_{\hat{\mathbf{u}}_{i,t-1}}(\mathbf{z}_i, \mathbf{a}_i, \mathbf{x}_i)\| + \beta_t \|\sigma_{\hat{\mathbf{u}}_{i,t-1}}(\mathbf{z}_i, \mathbf{a}_i, \mathbf{x}_i) \circ \omega_{\hat{\mathbf{u}}_{i,t-1}}(\mathbf{z}_i, \mathbf{a}_i, \mathbf{x}_i)\| \\ &\leq 2\beta_t \|\sigma_{\hat{\mathbf{u}}_{i,t-1}}(\mathbf{z}_i, \mathbf{a}_i, \mathbf{x}_i)\| = 2\beta_t \|\sigma_{h,i,t-1}\|. \end{aligned}$$

□

With the decomposable Assumption 6.2 on \mathbf{f}_i , $\sigma_{h,i,t-1}^2 \propto \mathbf{f}_{i(b)}^2(\mathbf{z}_i, \mathbf{a}_i) (\mathbf{f}_{i(c)}(U) - \mathbb{E}[\mathbf{f}_{i(c)}(U)])^2$ according to the proof of Theorem 4.1. $\mathbf{f}_{i(b)}()$ is learned with the variance of regression model $\phi()$, i.e. $\sigma_{\phi,i,t}()$.

Lemma B.2.

$$\|\mathbf{x}_{d,t} - \tilde{\mathbf{x}}_{d,t}\| \leq 2\beta_t M^{N_i} (2\beta_t L_{\sigma_g} + L_g)^{N_i} \sum_{j=0}^i (\sigma_{g,j,t-1}(\mathbf{z}_{j,t}) + \sigma_{\hat{\mathbf{u}}_{j,t-1}}).$$

Proof. We use $\mathbf{g}_i(\mathbf{z}_{i,t}, \hat{\mathbf{u}}_{i,t})$ to represent $\mathbf{g}_i(\mathbf{z}_{i,t}, \mathbf{a}_{i,t}, \hat{\mathbf{u}}_{i,t})$ because we assume the actions to be the same for the process generating $\mathbf{x}_{i,t}$ and $\tilde{\mathbf{x}}_{i,t}$. Similarly, $\mu_{g,i,t-1}(\tilde{\mathbf{z}}_{i,t}, \tilde{\mathbf{u}}_{i,t}) = \mu_{g,i,t-1}(\tilde{\mathbf{z}}_{i,t}, \tilde{\mathbf{a}}_{i,t}, \tilde{\mathbf{u}}_{i,t})$, $\sigma_{g,i,t-1}(\tilde{\mathbf{z}}_{i,t}, \tilde{\mathbf{u}}_{i,t}) = \sigma_{g,i,t-1}(\tilde{\mathbf{z}}_{i,t}, \tilde{\mathbf{a}}_{i,t}, \tilde{\mathbf{u}}_{i,t})$.

We use the reparameterization trick, and write $\tilde{\mathbf{x}}_{i,t}$ as

$$\tilde{\mathbf{x}}_{i,t} = \tilde{\mathbf{g}}_i(\tilde{\mathbf{z}}_{i,t}, \tilde{\mathbf{u}}_{i,t}) = \mu_{g,i,t-1}(\tilde{\mathbf{z}}_{i,t}, \tilde{\mathbf{u}}_{i,t}) + \beta_t \sigma_{g,i,t-1}(\tilde{\mathbf{z}}_{i,t}, \tilde{\mathbf{u}}_{i,t}) \circ \omega_{g,i,t-1}(\tilde{\mathbf{z}}_{i,t}, \tilde{\mathbf{u}}_{i,t}).$$

Here $|\boldsymbol{\omega}_{g,i,t-1}(\tilde{\mathbf{z}}_i, \tilde{\mathbf{u}}_{i,t})| \leq 1$. Hence, we have

$$\begin{aligned}
\|\mathbf{x}_{i,t} - \tilde{\mathbf{x}}_{i,t}\| &= \|\mathbf{g}_i(\mathbf{z}_{i,t}, \hat{\mathbf{u}}_{i,t}) - \boldsymbol{\mu}_{g,i,t-1}(\tilde{\mathbf{z}}_i, \tilde{\mathbf{u}}_{i,t}) - \beta_t \boldsymbol{\sigma}_{g,i,t-1}(\tilde{\mathbf{z}}_i, \tilde{\mathbf{u}}_{i,t}) \boldsymbol{\omega}_{g,i,t-1}(\tilde{\mathbf{z}}_i, \tilde{\mathbf{u}}_{i,t})\| \\
&= \|\mathbf{g}_i(\tilde{\mathbf{z}}_i, \tilde{\mathbf{u}}_{i,t}) - \boldsymbol{\mu}_{g,i,t-1}(\tilde{\mathbf{z}}_i, \tilde{\mathbf{u}}_{i,t}) - \beta_t \boldsymbol{\sigma}_{g,i,t-1}(\tilde{\mathbf{z}}_i, \tilde{\mathbf{u}}_{i,t}) \boldsymbol{\omega}_{g,i,t-1}(\tilde{\mathbf{z}}_i, \tilde{\mathbf{u}}_{i,t}) + \mathbf{g}_i(\mathbf{z}_{i,t}, \hat{\mathbf{u}}_{i,t}) - \mathbf{g}_i(\tilde{\mathbf{z}}_i, \tilde{\mathbf{u}}_{i,t})\| \\
&\leq \|\mathbf{g}_i(\tilde{\mathbf{z}}_i, \tilde{\mathbf{u}}_{i,t}) - \boldsymbol{\mu}_{g,i,t-1}(\tilde{\mathbf{z}}_i, \tilde{\mathbf{u}}_{i,t})\| + \|\beta_t \boldsymbol{\sigma}_{g,i,t-1}(\tilde{\mathbf{z}}_i, \tilde{\mathbf{u}}_{i,t}) \boldsymbol{\omega}_{g,i,t-1}(\tilde{\mathbf{z}}_i, \tilde{\mathbf{u}}_{i,t})\| \\
&\quad + \|\mathbf{g}_i(\mathbf{z}_{i,t}, \hat{\mathbf{u}}_{i,t}) - \mathbf{g}_i(\tilde{\mathbf{z}}_i, \tilde{\mathbf{u}}_{i,t})\| \\
&\stackrel{\zeta_1}{\leq} \beta_t \|\boldsymbol{\sigma}_{g,i,t-1}(\tilde{\mathbf{z}}_i, \tilde{\mathbf{u}}_{i,t})\| + \beta_t \|\boldsymbol{\sigma}_{g,i,t-1}(\tilde{\mathbf{z}}_i, \tilde{\mathbf{u}}_{i,t})\| + L_{\mathbf{g}_i} \|\mathbf{z}_{i,t}; \hat{\mathbf{u}}_{i,t}] - [\tilde{\mathbf{z}}_i, \tilde{\mathbf{u}}_{i,t}]\| \\
&= 2\beta_t \|\boldsymbol{\sigma}_{g,i,t-1}(\mathbf{z}_i, \hat{\mathbf{u}}_{i,t}) + \boldsymbol{\sigma}_{g,i,t-1}(\tilde{\mathbf{z}}_i, \tilde{\mathbf{u}}_{i,t}) - \boldsymbol{\sigma}_{g,i,t-1}(\mathbf{z}_i, \hat{\mathbf{u}}_{i,t})\| + L_{\mathbf{g}_i} \|\mathbf{z}_{i,t}; \hat{\mathbf{u}}_{i,t}] - [\tilde{\mathbf{z}}_i, \tilde{\mathbf{u}}_{i,t}]\| \\
&\stackrel{\zeta_2}{\leq} 2\beta_t \left(\|\boldsymbol{\sigma}_{g,i,t-1}(\mathbf{z}_i, \hat{\mathbf{u}}_{i,t})\| + L_{\boldsymbol{\sigma}_{g,i}} \|\mathbf{z}_{i,t}; \hat{\mathbf{u}}_{i,t}] - [\tilde{\mathbf{z}}_i, \tilde{\mathbf{u}}_{i,t}]\| \right) + L_{\mathbf{g}_i} \|\mathbf{z}_{i,t}; \hat{\mathbf{u}}_{i,t}] - [\tilde{\mathbf{z}}_i, \tilde{\mathbf{u}}_{i,t}]\| \\
&= 2\beta_t \boldsymbol{\sigma}_{g,i,t-1}(\mathbf{z}_i, \hat{\mathbf{u}}_{i,t}) + (2\beta_t L_{\boldsymbol{\sigma}_{g,i}} + L_{\mathbf{g}_i}) \|\mathbf{z}_{i,t}; \hat{\mathbf{u}}_{i,t}] - [\tilde{\mathbf{z}}_i, \tilde{\mathbf{u}}_{i,t}]\| \\
&\leq 2\beta_t \boldsymbol{\sigma}_{g,i,t-1}(\mathbf{z}_i, \hat{\mathbf{u}}_{i,t}) + (2\beta_t L_{\boldsymbol{\sigma}_{g,i}} + L_{\mathbf{g}_i}) \|\mathbf{z}_{i,t} - \tilde{\mathbf{z}}_i, t\| + (2\beta_t L_{\boldsymbol{\sigma}_{g,i}} + L_{\mathbf{g}_i}) \|\hat{\mathbf{u}}_{i,t} - \tilde{\mathbf{u}}_{i,t}\| \\
&\stackrel{\zeta_3}{\leq} 2\beta_t \boldsymbol{\sigma}_{g,i,t-1}(\mathbf{z}_i, \hat{\mathbf{u}}_{i,t}) + (2\beta_t L_{\boldsymbol{\sigma}_{g,i}} + L_{\mathbf{g}_i}) \|\mathbf{z}_{i,t} - \tilde{\mathbf{z}}_i, t\| + 2\beta_t (2\beta_t L_{\boldsymbol{\sigma}_{g,i}} + L_{\mathbf{g}_i}) \boldsymbol{\sigma}_{\hat{\mathbf{u}}_{i,t-1}} \\
&= 2\beta_t \boldsymbol{\sigma}_{g,i,t-1}(\mathbf{z}_i, \hat{\mathbf{u}}_{i,t}) + 2\beta_t (2\beta_t L_{\boldsymbol{\sigma}_{g,i}} + L_{\mathbf{g}_i}) \boldsymbol{\sigma}_{\hat{\mathbf{u}}_{i,t-1}} + (2\beta_t L_{\boldsymbol{\sigma}_{g,i}} + L_{\mathbf{g}_i}) \sum_{j \in \text{pa}(i)} \|\mathbf{x}_{j,t} - \tilde{\mathbf{x}}_{j,t}\| \\
&\leq 2\beta_t \boldsymbol{\sigma}_{g,i,t-1}(\mathbf{z}_i, \hat{\mathbf{u}}_{i,t}) + 2\beta_t (2\beta_t L_{\boldsymbol{\sigma}_g} + L_{\mathbf{g}}) \boldsymbol{\sigma}_{\hat{\mathbf{u}}_{i,t-1}} + (2\beta_t L_{\boldsymbol{\sigma}_g} + L_{\mathbf{g}}) \sum_{j \in \text{pa}(i)} \|\mathbf{x}_{j,t} - \tilde{\mathbf{x}}_{j,t}\| \\
&\stackrel{\zeta_4}{\leq} 2\beta_t \boldsymbol{\sigma}_{g,i,t-1}(\mathbf{z}_i, \hat{\mathbf{u}}_{i,t}) + 2\beta_t (2\beta_t L_{\boldsymbol{\sigma}_g} + L_{\mathbf{g}}) \boldsymbol{\sigma}_{\hat{\mathbf{u}}_{i,t-1}} \\
&\quad + (2\beta_t L_{\boldsymbol{\sigma}_g} + L_{\mathbf{g}}) \sum_{j \in \text{pa}(i)} 2\beta_t M^{N_j} (2\beta_t L_{\boldsymbol{\sigma}_g} + L_{\mathbf{g}})^{N_j} \sum_{h=0}^j (\boldsymbol{\sigma}_{g,h,t-1}(\mathbf{z}_{h,t}) + \boldsymbol{\sigma}_{\hat{\mathbf{u}}_{h,t-1}}) \\
&\leq 2\beta_t M^{N_i} (2\beta_t L_{\boldsymbol{\sigma}_g} + L_{\mathbf{g}})^{N_i} \sum_{j=0}^i (\boldsymbol{\sigma}_{g,j,t-1}(\mathbf{z}_{j,t}) + \boldsymbol{\sigma}_{\hat{\mathbf{u}}_{j,t-1}})
\end{aligned}$$

In steps ζ_1 and ζ_2 , we rely on the calibrated uncertainty and Lipschitz dynamics; in step ζ_2 , we also apply the triangle inequality; step ζ_3 is by Lemma B.1; ζ_4 applies the inductive hypothesis. \square

Theorem 6.1 Consider the optimization problem in (6), with the SCM satisfying Assumptions 6.1-6.3, where \mathcal{G} is known but \mathbf{F} is unknown. Then with probability at least $1 - \alpha$, the cumulative regret of Algorithm 1 is bounded by

$$R_T \leq \mathcal{O}(L_T M^N d \sqrt{T \gamma_T}).$$

Proof. The cumulative regret is

$$R_T = \sum_{t=1}^T \left[\mathbb{E}[y|\mathbf{a}^*] - \mathbb{E}[y|\mathbf{a}_{\cdot,t}] \right].$$

At step t , the instantaneous regret is r_t . By applying Lemma B.2, r_t is bounded by

$$\begin{aligned}
r_t &= \mathbb{E}[y|\mathbf{F}, \mathbf{a}^*] - \mathbb{E}[y|\mathbf{F}, \mathbf{a}_{:,t}] \\
&\leq \mathbb{E}[y_t|\tilde{\mathbf{F}}, \mathbf{a}_{:,t}] - \mathbb{E}[y_t|\mathbf{F}, \mathbf{a}_{:,t}] \\
&= \mathbb{E}[\|\mathbf{x}_{i,t} - \tilde{\mathbf{x}}_{i,t}\| | \mathbf{a}_{:,t}] \\
&\leq 2\beta_t M^N (2\beta_t L_{\sigma_g} + L_g)^N \mathbb{E} \left[\sum_{i=0}^d \|\sigma_{g,i,t-1}(\mathbf{z}_{i,t})\| + \|\sigma_{\hat{\mathbf{u}}_{i,t-1}}\| \right]
\end{aligned}$$

Here $L_t = 2\beta_t(2\beta_t L_{\sigma_g} + L_g)^N$. Thus,

$$\begin{aligned}
r_t^2 &\leq L_t^2 M^{2N} \left(\mathbb{E} \left[\sum_{i=0}^d \|\sigma_{g,i,t-1}(\mathbf{z}_{i,t})\| + \|\sigma_{\hat{\mathbf{u}}_{i,t-1}}\| \right] \right)^2 \\
&\leq 2dL_t^2 M^{2N} \mathbb{E} \left[\sum_{i=0}^d \|\sigma_{g,i,t-1}(\mathbf{z}_{i,t})\|_2^2 + \|\sigma_{\hat{\mathbf{u}}_{i,t-1}}\|_2^2 \right]
\end{aligned}$$

We define R_T^2 as

$$\begin{aligned}
R_T^2 &= \left(\sum_{t=1}^T r_t \right)^2 \leq T \sum_{t=1}^T r_t^2 \\
&\leq 2dT L_T^2 M^{2N} \sum_{t=1}^T \mathbb{E} \left[\sum_{i=0}^d \|\sigma_{g,i,t-1}(\mathbf{z}_{i,t})\|_2^2 + \|\sigma_{\hat{\mathbf{u}}_{i,t-1}}\|_2^2 \right] \\
&= 2dT L_T^2 M^{2N} \Gamma_T.
\end{aligned}$$

Here,

$$\begin{aligned}
\Gamma_T &= \max_{(\mathbf{z}, \mathbf{a}, \hat{\mathbf{u}}) \in \mathcal{Z} \times \mathcal{A} \times \hat{\mathcal{U}}} \sum_{t=1}^T \sum_{i=0}^d \left[\|\sigma_{i,t-1}(\mathbf{z}_{i,t}, \mathbf{a}_{i,t})\|_2^2 + \|\sigma_{\hat{\mathbf{u}}_{i,t-1}}\|_2^2 \right] \\
&\leq \max_{A, \hat{U}} \sum_{t=1}^T \sum_{i=0}^d \left[\|\sigma_{i,t-1}(\mathbf{z}_{i,t}, \mathbf{a}_{i,t})\|_2^2 + \|\sigma_{\hat{\mathbf{u}}_{i,t-1}}\|_2^2 \right] \\
&\leq \sum_{i=0}^d \max_{A_i, \hat{U}_i} \sum_{t=1}^T \left[\|\sigma_{i,t-1}(\mathbf{z}_{i,t}, \mathbf{a}_{i,t})\|_2^2 + \|\sigma_{\hat{\mathbf{u}}_{i,t-1}}\|_2^2 \right] \\
&\leq \sum_{i=0}^d \max_{A_i, \hat{U}_i} \sum_{t=1}^T \left[\sum_{l=1}^{d_i} \|\sigma_{i,t-1}(\mathbf{z}_{i,t}, \mathbf{a}_{i,t}, l)\|_2^2 + \|\sigma_{\hat{\mathbf{u}}_{i,t-1}}\|_2^2 \right] \\
&\leq \sum_{i=0}^d \frac{2}{\ln(1 + \rho_i^{-2})} \gamma_{i,T} \\
&= \mathcal{O}(d\gamma_T).
\end{aligned}$$

Here ζ_1 is due to the upper bound of the information gain [22], and γ_T will often scale sublinearly in T [23]. Therefore,

$$R_T^2 \leq 2dT L_T^2 M^{2N} d\mathcal{O}(d\gamma_T).$$

And,

$$R_T \leq \mathcal{O}(L_T M^N d \sqrt{T \gamma_T}).$$

This completes the proof of the theorem. □

C Additional Experimental Results

C.1 Dropwave Dataset

The structure of Dropwave is given in Figure 8. Here we use σ to control the noise level in the generated datasets. Figure 9 gives the average reward values achieved by the competing algorithms using four different random seeds in the code, and shadows are the scaled standard deviations of the four results. In each round, the size of the observation on the true model equals the round number.

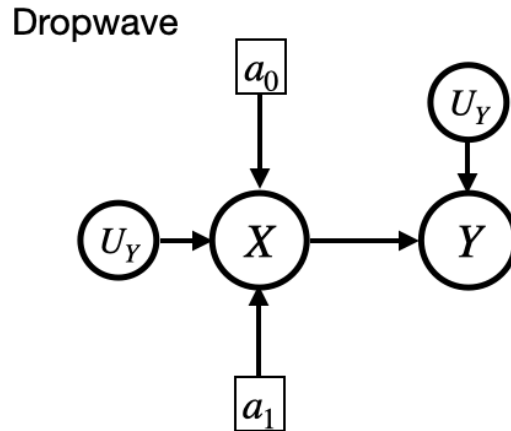


Figure 8: Graph structure of Dropwave dataset.

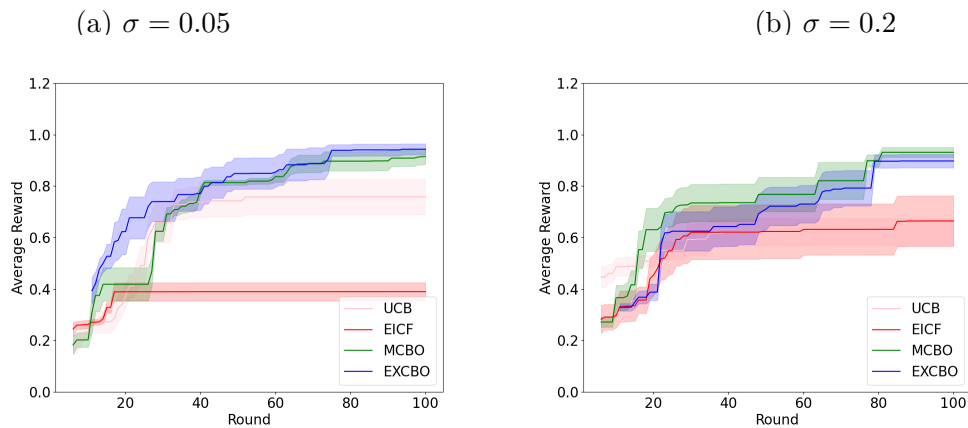


Figure 9: Results of Dropwave at different noise levels.

Figure 9-(a) presents the results at $\sigma = 0.05$. It can be observed clearly that EXCBO achieves the best reward at nearly all rounds. In Figure 9-(b), EXCBO achieves equal or better rewards

than the other methods before round 40. In addition, EXCBO performs better than both UCB and EICF at all rounds. Though MCBO achieves the best performance after round 40, MCBO consumes much more CPU time (10+ times) compared to the other three methods that do not rely on neural networks.

C.2 Rosenbrock Dataset

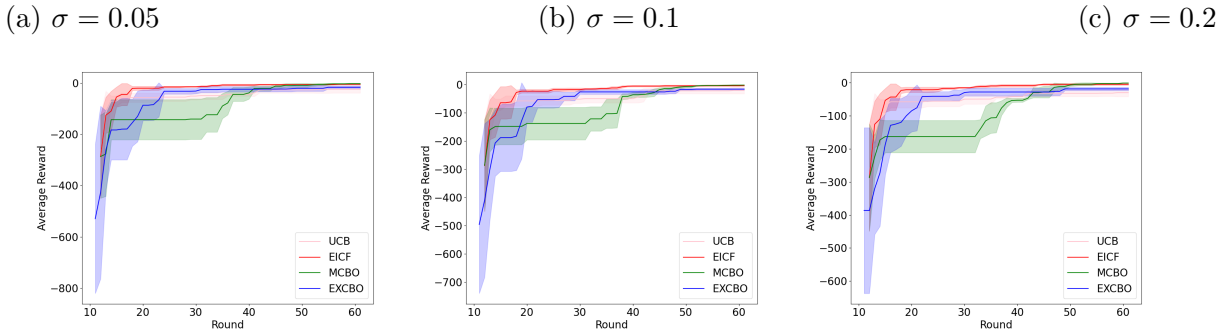


Figure 10: Results of Rosenbrock at different noise levels.

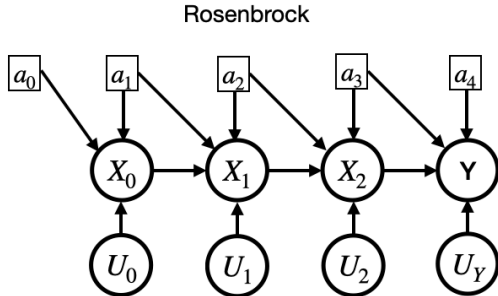


Figure 11: Graph structure of Rosenbrock dataset.

The graph structure of the Rosenbrock Dataset is shown in Figure 11. There are four endogenous nodes in Rosenbrock, i.e., $\{X_i\}_{i=0}^2 \cup \{Y\}$, and Y is the target variable. There is at least one action node assigned to each endogenous node. Similar to Dropwave, the exogenous distributions for X_0, X_1, X_2 , and Y are two-component Gaussian Mixture models given by (9). The results of Rosenbrock are shown in Figure 10. As shown in the plots on different noise levels, EICF nearly performs the best in all rounds. EXCBO performs better than MCBO between rounds 20 and 40. MCBO performs better than UCB after round 20. In summary, MCBO achieves comparable results with other methods on Rosenbrock.

C.3 Additional Experimental Analysis on EXCBO

This section presents an additional empirical analysis of the proposed EXCBO algorithm.

Dropwave Dataset

The graph structure of the Dropwave Dataset is given by Figure 8. There are two endogenous nodes in Dropwave, i.e., X and the target node Y . There are two action nodes associated with X , a_0 and a_1 . Here $a_0, a_1 \in [0, 1]$, $X = \sqrt{(c_1 \cdot a_0 - c_2)^2 + (c_1 \cdot a_1 - c_2)^2} + \epsilon_X$, $c_1 = 10.24, c_2 = 5.12$,

and $Y = (1.0 + \cos(12.0X))/(2.0 + 0.5X^2) + \epsilon_Y$, $\epsilon_X, \epsilon_Y \sim \mathcal{N}(0, \sigma)$. We change the value of σ to generate data samples with different noise levels.

Figure 12 shows the average reward/objective values achieved by the proposed EXCBO algorithm in different rounds. The surrogate model is initialized with 20 samples. The shadow stands for the magnitude of the standard deviation of the reward values from nine different random seeds in the code. The figure shows that the reward values increase with more data points in the training set. Moreover, we notice that the algorithm achieves improved results at higher noise levels in the datasets.

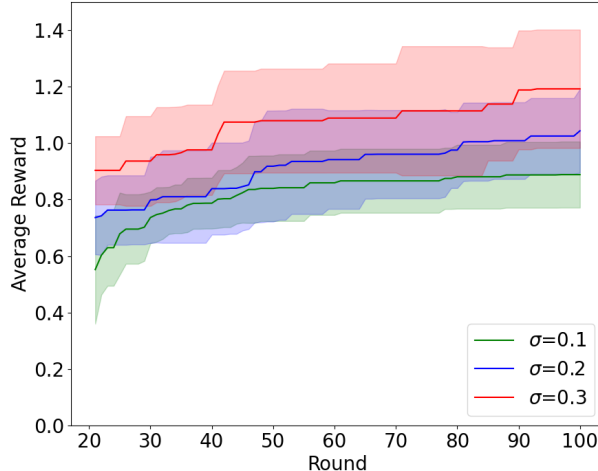


Figure 12: Reward values achieved by EXCBO in different rounds on Dropwave. The results are on three different Gaussian noise levels with $\sigma = \{0.1, 0.2, 0.3\}$.

We performed a further investigation on the surrogate model learned by the EXCBO algorithm using the Dropwave dataset at $\sigma = 0.1$. The algorithm is initialized with 30 data samples, and then we plot the learned surrogate function from X and Y at step $t = 30$. Figure 13 shows the surrogate model mean and scaled standard derivation at $t = 0$ and $t = 30$. Plot (c) in Figure 13 shows the data points sampled from the ground truth model, and it indicates that the dataset is very noisy. As shown in the plots, at $t = 0$ data points are evenly sampled in the value span of X . At $t = 30$, we can see that the probabilistic surrogate model drives the EXCBO algorithm to obtain more samples around the optimal location. We further notice that the variance of the surrogate decreases at the locations with dense data samples. Plots (a) and (b) show that the surrogate model employed by EXCBO improves the learning of the unknown function as well as the estimation of uncertain along with more observations.

Rosenbrock Dataset

Figure 11 shows the graph structure of the Rosenbrock dataset. Figure 14 shows the average reward values attained by the proposed EXCBO algorithm with nine different random seeds. The surrogate model is initialized with 20 samples. As shown in the figure, similar to Dropwave the reward values increase with more observational data points in the training set. However, different from the result of Dropwave, the variance of the reward value decreases significantly with more training data samples. Another difference from Dropwave is that the performance of the EXCBO algorithm is barely affected by the noise level in the dataset.

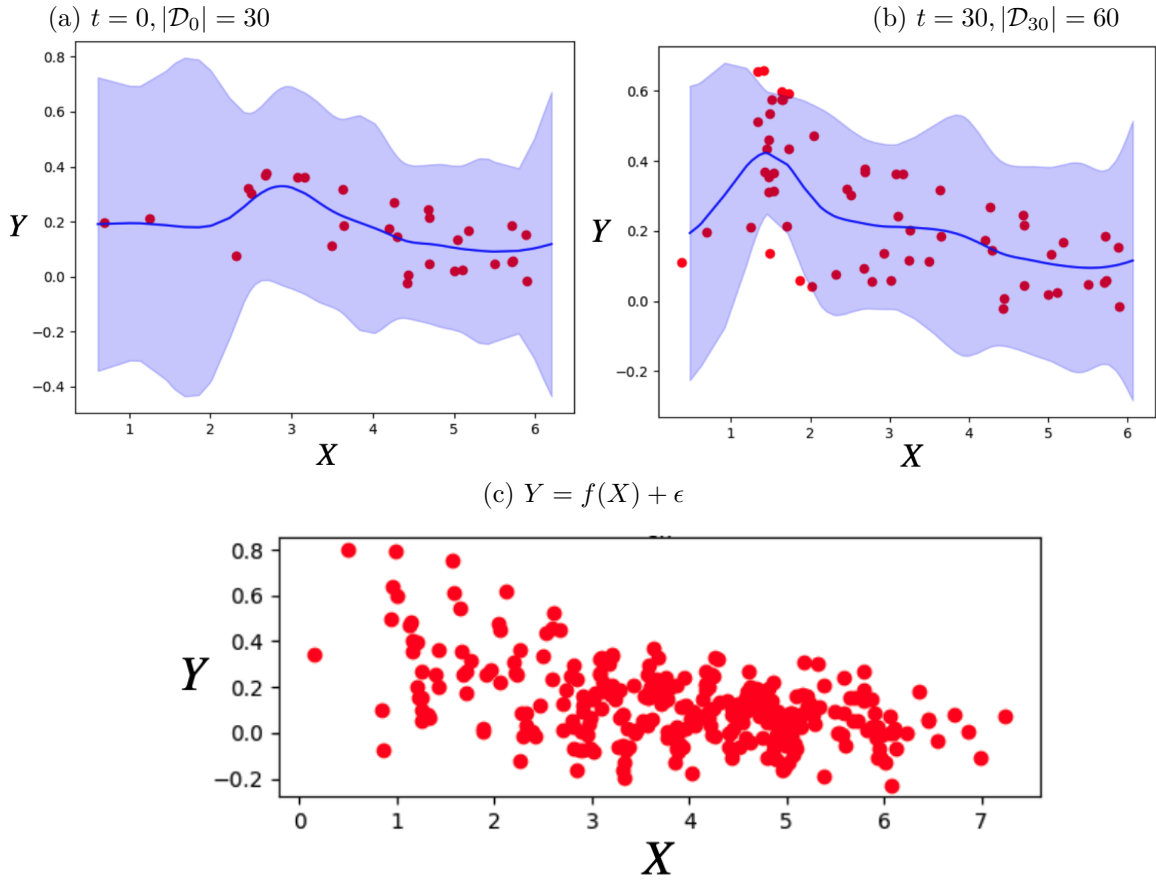


Figure 13: Surrogate model of EXCBO on Dropwave. The blue curve is the surrogate mean, and the blue shadow stands for the scaled standard derivation of the surrogate model; red points are samples from the ground truth model. (a) At step $t = 0$, the model is initialized with 30 samples; (b) At step $t = 30$, more observations are around the optimal location; (c) Samples from the ground truth function of Y .

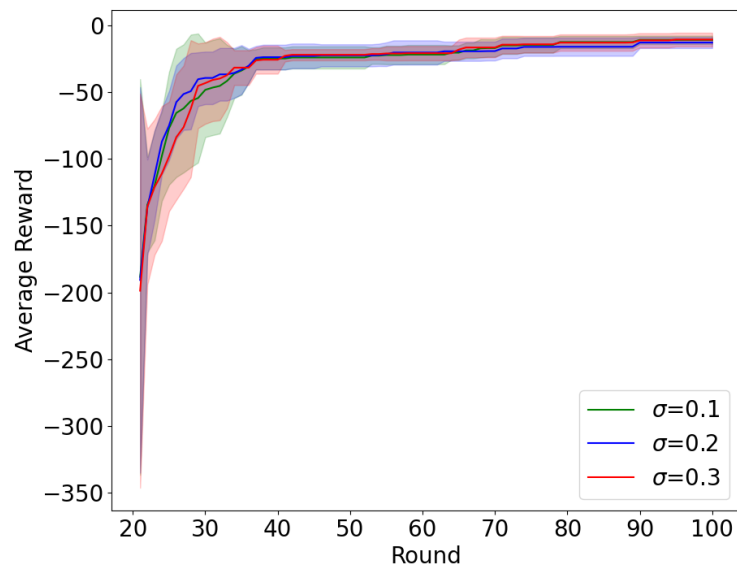


Figure 14: Reward values achieved by EXCBO in different rounds on Rosenbrock. The results are on three different Gaussian noise levels with $\sigma = \{0.1, 0.2, 0.3\}$.